

Spring 5-17-2013

Cellular Mechanisms of Pathogenesis of *Pseudomonas Aeruginosa*

Omar Jorge Castillo

Follow this and additional works at: https://scholarworks.uttyler.edu/biology_grad

 Part of the [Biology Commons](#)

Recommended Citation

Castillo, Omar Jorge, "Cellular Mechanisms of Pathogenesis of *Pseudomonas Aeruginosa*" (2013). *Biology Theses*. Paper 1.
<http://hdl.handle.net/10950/113>

This Thesis is brought to you for free and open access by the Biology at Scholar Works at UT Tyler. It has been accepted for inclusion in Biology Theses by an authorized administrator of Scholar Works at UT Tyler. For more information, please contact tbianchi@uttyler.edu.

CELLULAR MECHANISMS OF PATHOGENESIS OF
PSEUDOMONAS AERUGINOSA

by

OMAR JORGE CASTILLO

A thesis submitted in partial fulfillment
of the requirements for the degree of
Master of Science
Department of Biology

Ali Azghani, Ph.D., Committee Chair

College of Arts and Sciences

The University of Texas at Tyler
May 2013

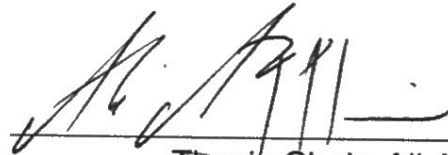
The University of Texas at Tyler
Tyler, Texas

This is to certify that the Master's Thesis of

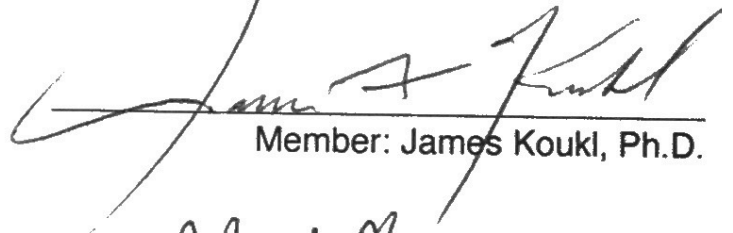
OMAR JORGE CASTILLO

has been approved for the thesis requirement on
April 10th, 2013
for the Master of Science degree

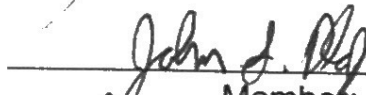
Approvals:



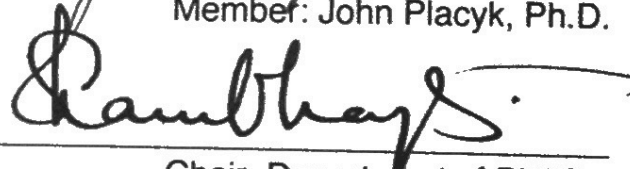
Thesis Chair: Ali Azghani, Ph.D.



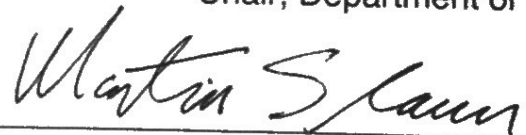
Member: James Koukl, Ph.D.



Member: John Placyk, Ph.D.



Chair, Department of Biology



Dean, College of Arts and Sciences

© Copyright by Omar Jorge Castillo 2013
All rights reserved

Acknowledgments

I would like to thank the many people that have helped me through this thesis. Foremost I extend my heartfelt gratitude to my advisor Prof. Ali Azghani for his continuous support; his enthusiasm, patience, scholarship and immense knowledge have made this thesis possible. I hope that someday, I can in turn pass on the research values and inspiration that he has given me.

I would also like to thank my committee members Profs. Jim Koukl and John Placyk, who provided encouraging and constructive feedback; it is no easy task reviewing a thesis. Jessica Coleman for all her support during this endeavor, a light of hope in the darkness.

My appreciation also extends to the numerous graduate and undergraduate students that broke the monotony of lab work and provided comedic relief when it was much needed. I was also very fortunate to be able to teach numerous undergraduates, and at the same time they taught me as well.

Finally I would like to thank those who are closest to me whose support was invaluable. Byung Yun my best and most reliable friend for the past 18 years. Most of all I would like to thank my family, and especially my parents for their unrivaled support and love. They have truly been an inspiration and a role model.

Table of Contents

List of Figures	ii
Chapter One	
Abstract: Epidermal Growth Factor Receptor Activation by <i>Pseudomonas aeruginosa</i> and its Role in Pulmonary Epithelial Injury.....	iv
Introduction	1
Methods	7
Results	12
Discussion	30
References	36
Chapter Two	
Abstract: <i>Pseudomonas aeruginosa</i> Elastase Disruption of Tight Junctions via MAPK Signaling Pathway	43
Introduction	44
Methods	48
Results	53
Discussion	67
References	71

List of Figures

Chapter One

Figure 1	Schematic representation of tight junctions proteins	4
Figure 2	PE disrupts epithelial permeability as measured by TER.....	13
Figure 3	Effects of EGFR inhibition and PE exposure on tight junction integrity as measured by TER	14
Figure 4A	PE phosphorylates epidermal growth factor receptor (EGFR Tyr-1068) within 5 minutes of apical exposure	16
Figure 4B	Densitometric evaluation of phosphorylation of EGFR relative to control after exposure to 2 U/mL of PE.....	16
Figure 5A	Inhibition of EGFR decreased ZO-1 protein degradation after PE exposure	18
Figure 5B	Densitometric analysis of ZO-1 protein levels after exposure to PE, inhibition of EGFR diminished protein loss	18
Figure 6	Immunofluorescence microscopy of tight junction protein ZO-1 of Calu-3 cells exposed to PE.....	20
Figure 7A	EGFR inhibition prevents occludin translocation in a time dependent manner	22
Figure 7B	EGFR inhibition sustained occludin protein levels after exposure to 2U of PE	22
Figure 8	Immunofluorescence microscopy images of tight junction protein occludin exposed to PE	24
Figure 9	Representative photomicrographs of occludin and F-actin obtained by fluorescent microscopy after exposure to PE.....	27

Figure 10	Representative photomicrographs of ZO-1 and F-actin obtained by immunofluorescence of Calu-3 monolayers after exposure to PE	28
-----------	------------------------------------------------------------------------------------------------------------------------------------	----

Chapter Two

Figure 1	Schematic representation of several signaling pathways activated by the epidermal growth factor receptor	47
Figure 2	Inhibition of MAPK attenuated <i>Pseudomonas</i> elastase (PE) induced disruption of tight junction integrity as measured by TER.....	54
Figure 3A	Representative western blot analysis of confluent Calu-3 monolayers exposed for 5 minutes to 2 U/mL of PE	56
Figure 3B	Quantification of phosphorylation levels of ERK 1/2 protein in response to PE	56
Figure 4A	Inhibition of EGFR and ERK decreased ZO-1 protein loss in Calu-3 cell lysates after PE exposure.....	57
Figure 4B	Densitometry of ZO-1 protein expression after exposure to PE, inhibition of ERK diminished protein loss.....	58
Figure 5	Immunofluorescence micrographs of tight junction protein ZO-1 of Calu-3 monolayers after exposure to PE (2 U/mL) for 1 hour ..	60
Figure 6	Immunofluorescence micrographs of tight junction protein occludin of Calu-3 cells exposed to elastase for 1 hour	62
Figure 7	Representative micrographs obtained by immunofluorescence staining of occludin and F-actin	65
Figure 8	Representative fluorescent micrographs of ZO-1 and F-actin during PE exposure	66

Abstract

Epidermal Growth Factor Receptor Activation by *Pseudomonas aeruginosa* Elastase and its Role in Pulmonary Epithelial Injury

Omar J. Castillo

Thesis Chair: Ali Azghani, Ph.D.

The University of Texas at Tyler
Spring 2013

Epithelial permeability is distorted by *Pseudomonas aeruginosa* elastase (PE) and changes in barrier function are caused by disruption of tight junction (TJ) proteins occludin, zonula occludens (ZO)-1 and alterations of the cytoskeleton. Increase in paracellular permeability is caused, in part, by activation of cellular signaling transduction pathways. The exact signaling mechanisms that lead to epithelial disruption are not yet fully understood. I sought to evaluate whether PE exposure can activate the epidermal growth factor receptor (EGFR) and what role, it plays in TJ disruption. My results indicate that inhibition of EGFR attenuated PE induced disruptive changes in expression of TJ proteins occludin and ZO-1. Elastase also caused morphological changes in TJ proteins within 1 hour. Occludin was translocated from the membrane and ZO-1 was delocalized from the cellular periphery. Structural changes in TJ proteins correlated with decreased transepithelial electrical resistance measurements, which is indicative

of decreased barrier function. I propose that PE induces changes in TJ structure and function by an EGFR dependent mechanism.

Chapter One

Introduction

Pseudomonas aeruginosa is a ubiquitous, Gram-negative, opportunistic bacterium, which can cause acute pneumonia, chronic lung infection and bronchiectasis in patients with cystic fibrosis (CF). The lack of a vaccine and an effective long-term antibiotic therapy makes management of this pathogen incredibly challenging. In CF populations, pulmonary colonization by *Pseudomonas* is achieved by numerous events; eminent among them is inadequate function of mucociliary motility due to viscid dehydrated mucus secretions, which impair clearance of the bacterium from the lungs [1,2]. *In vivo* studies indicate that *P. aeruginosa* rarely directly adheres to the airway epithelium [3], instead it preferentially resides as biofilms in CF lungs [1,4], where it can secrete a number of virulence factors onto the pulmonary epithelium. Thus, it is likely that these secreted metabolites are responsible for disruption of the epithelium and subsequent inflammation and edema. *Pseudomonas aeruginosa* virulence factors include extracellular toxins that aid in the pulmonary infection; they include elastase, exotoxin A, exoenzyme S, pyocyanin pigment and several alkaline proteases [5-8].

Once pulmonary colonization is achieved, *P. aeruginosa* perturbs the integrity of the airway epithelial lining [7], which relies on an effective cell-cell and cell-matrix interactions [9] in order to maintain epithelial integrity. One of the early destructive effects of *P. aeruginosa* is, its ability to increase paracellular epithelial permeability to ions and macromolecules [10]. The pulmonary epithelium consists of a series of junctional complexes, which include: tight junctions, desmosomes, gap junctions, and adherence junctions, each with a diverse structure and a unique role [11]. Of particular interest is the furthestmost layer in the epithelium which is composed of tight junction (TJ) proteins, where they serve as gatekeepers to paracellular permeability and help maintain cell polarity [12]. Bacterial mediated disruptions in TJ structure and function compromise physiological and defensive role of the epithelia and facilitate bacterial systemic dissemination to other tissues [7]. Furthermore, considering the fact that the basolateral domain of the epithelia is extremely sensitive to cytotoxins of *P. aeruginosa* [13], it is inferred that increased epithelial permeability renders the lungs more susceptible to pulmonary injury [14].

Thus, maintaining the structure and function of TJ proteins is essential to prevent and if necessary, combat infection. When visualized with freeze-fracture electron microscopy this junctional complex appears as a series of independent sealing strands in pulmonary epithelia [15,16]. Notable TJ complex proteins include claudins, occludins and several junction adhesion molecules. Prominent among these are the zonula occludens (ZO-1, ZO-2 and ZO-3) proteins, which

belong to the family of membrane-associated guanylate kinase homologs [17]. Within these proteins is ZO-1, a 225-kD protein that is found to be localized on the junctional complex region in a variety of epithelia [18]. Localized ZO-1 in the cellular periphery is closely associated with functional tight junctions [19]. As for ZO-1 function, it is a scaffolding/adapting protein that connects perijunctional actin filaments with transmembrane proteins of TJs, such as occludin [19,20]. The 65-kD transmembrane protein occludin spans the cell four times and contains two large extracellular COOH-terminal cytoplasmic domains that link to other occludins on adjacent cells via homophilic interactions [20,21]. Finally, claudins and occludins seal TJs by making homotypic interactions with neighboring cells (Figure 1) [21,22]. This dependency of the epithelial cell barrier upon proteins that have extracellular domains raises the possibility that TJs might be influenced by external factors that perturb protein structure and/or function.

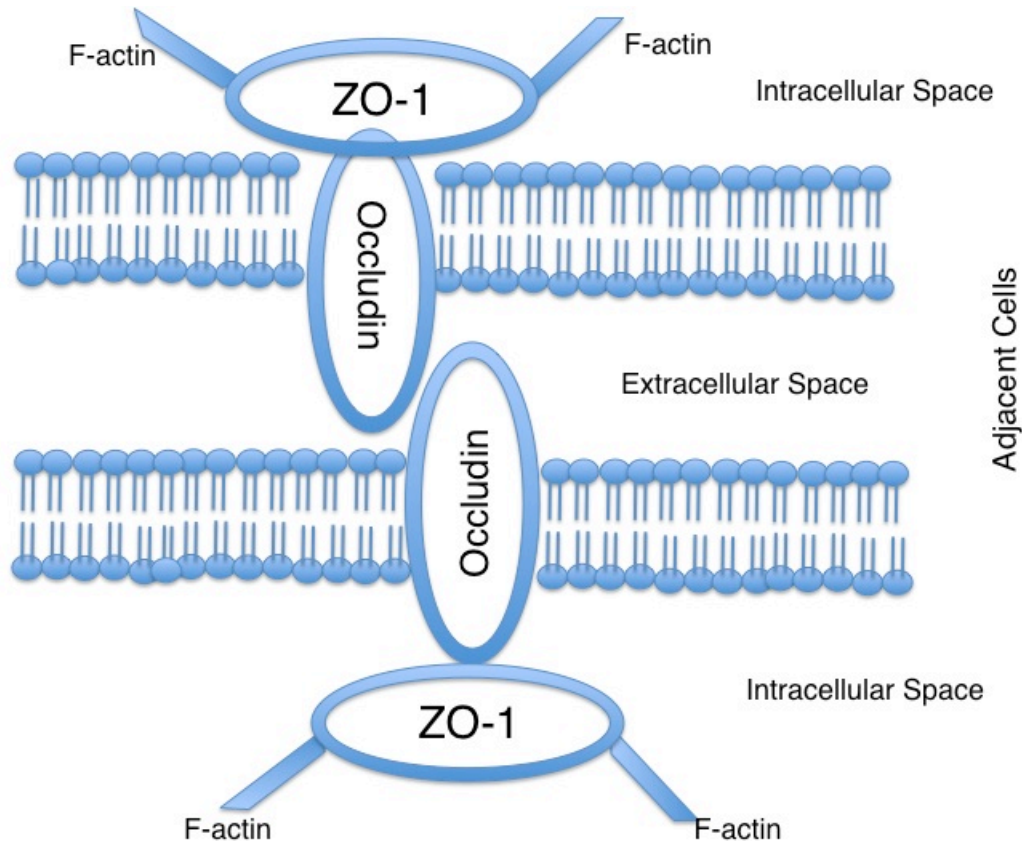


Figure 1. Schematic representation of tight junction proteins. Scaffolding adaptor protein ZO-1 links the cytoskeleton with the transmembrane protein occludin. Occludin is an essential component of TJs by linking with itself at the COOH-terminal cytoplasmic domains of adjacent cells.

One of the key virulence factors in *P. aeruginosa* infections is the zinc metalloproteinase elastase (PE) [23]. *Pseudomonas* elastase, also known as LasB, has proteolytic activity. It is involved in elastin destruction and induction of host cell signal transduction events [23-26]. In a gene knockout experiment, *Pseudomonas* lacking elastase were found to be less virulent and molecules cleared more easily from the lungs in mice models, with an observed dose-dependent destructive effect [7]. One study demonstrated that PE can induce protein kinase C (PKC) signaling, an event which resulted in decreased occludin functionality, leading to tight junction disruption and cytoskeletal alterations [24].

The molecular mechanisms through which *P. aeruginosa* accomplishes its early destructive effects on the epithelial barrier are poorly understood. Studies have indicated that PE increases paracellular permeability of pulmonary epithelia by either: cytoskeleton reorganization, depletion, or disconnection of F-actin from tight junctional proteins [7,24,27]. Others have suggested that disruption of the TJ complex might occur through activation of the mitogen-activated protein kinase (MAPK) pathway [26,28]. Since various intracellular signaling pathways are involved in the assembly, function and integrity of TJs [29-35], it is conceivable that PE utilizes specific host cells signaling mediators to modulate epithelial barrier function.

The epidermal growth factor receptor (EGFR) found in the superfamily of tyrosine kinase receptors is involved in regulation, differentiation and mitosis[29,30]. It is a transmembrane protein that exists in the plasma membrane as a monomer; once it is activated it undergoes ligand-induced dimerization, which leads to phosphorylation of one of several tyrosine kinase cytoplasmic domains. Activation of these intracellular tyrosine kinase residues can initiate stimulation of several signaling pathways [31-35]. A previous study from our laboratory with pulmonary fibroblasts (IMR90) cells demonstrated that PE phosphorylates tyrosine-1068 with a higher affinity than the rest of the tyrosine residues. This makes tyrosine-1068 the most likely target for phosphorylation by PE in Calu-3 cells.

Tight junctions are associated with various cell membrane and cytosol components. Their assembly and function are regulated by activation of several signal transduction pathways [24,36,38]. *In vivo* exposure of *Pseudomonas* elastase will first reach the apical layer [39], where histopathological studies have found that elastase disrupts the epithelium and increases lung epithelial permeability [10,25,40]. *In vitro* studies indicate that PE alters epithelial permeability by depleting TJ proteins occludin and ZO-1 in a dose and time dependent manner, however PE exposure does not change claudin expression [10,24].

I address the hypothesis that disruption of the cytoskeleton and TJ proteins by *Pseudomonas* elastase may occur through activation of EGFR and downstream signal transduction cascade of MAPK. I provide evidence indicating that alterations of the cytoskeleton and the TJ complex by *Pseudomonas* elastase occur through activation of EGFR and downstream signaling of MAPK.

Materials and Methods

Cell culture

Human bronchial adenocarcinoma epithelial cell lines, Calu-3 (ATCC), were used as an *in vitro* model of epithelial cell injury. Calu-3 cells were chosen due to their well-documented capacity to form tight junctions and their associated inter-cellular proteins that include occludin and ZO-1; and ability to form monolayers that are impermeable to ions and macromolecules [37,41]. Cells were cultured in RPMI-1640 (HyClone, South Logan, UT) and supplemented with 10% fetal bovine serum (Atlanta Biologicals, Lawrenceville, GA) and 1% L-glutamine (Cellgro, Herndon, VA). Cells were incubated at 37 °C in an atmosphere of 5% CO₂ and maintained with a penicillin (100 U/ml) and streptomycin (0.1 mg/ml) cocktail (BioWhittaker, Walkersville, MD). Cells were grown in 75cm² tissue culture flasks (Corning, Corning, NY) and were transferred at 80% confluency; all experiments were carried out between passage numbers 15-30. For epithelial permeability measurements, cells were seeded at a density of 1.0 x 10⁵ cells per insert, on a 6.5mm porous, polycarbonate tissue-culture transwell permeable insert (0.4 μm pore size and 0.33 cm², Costar, Lowell, MA) until they formed confluent monolayers. Before treatment, the cells were serum starved in RPMI-1640 with 1% L-glutamine for 12 hours.

Specific Inhibitors of Cell Signaling Pathways

To demonstrate involvement of EGFR activation and signaling through an EGFR/MAPK signaling pathway, I utilized a specific EGFR tyrosine kinase

inhibitor, AG1478 (Calbiochem, La Jolla, CA). A MEK1/2 inhibitor U0126 (Calbiochem, La Jolla, CA) was used to block the activation of the extracellular signal-regulated kinase (ERK1/2) arm of MAPK signaling pathway [42]. Cells were pre-treated for 30 minutes with either a 1 μ M dilution of AG1478 or a 25 μ M dilution of U0126, prior to being exposed to elastase. As a positive control I treated cells with epidermal growth factor (Sigma, St. Louis, MO) for 1 hour. All inhibitors were diluted in RPMI-1640 with 1% L-glutamine.

Bacterial Elastase

I utilized purified *P. aeruginosa* elastase (Elastin Product Co, Owensville, MO) and applied it apically on Calu-3 monolayers at a concentration of 2 U/mL. On average a dose of 2 U/mL is found in the lungs of patients infected with *P. aeruginosa* based on antigen quantification from sputum samples [27]. Elastase had its purity and enzymatic activity confirmed using an elastin-fluorescein assay as directed by the manufacturer.

Transepithelial Electrical Resistance

In order to quantitatively assess changes in paracellular permeability I measured changes in transepithelial electrical resistance (TER). Changes in TER were measured with chopstick-like electrodes placed in the apical and basal domains of confluent monolayers connected to a voltmeter (Millicell ERS, Billerica, MA). Readings were taken before and during apical treatment of the monolayers to evaluate their electrical resistance and tight junction integrity. Electrical resistance was calculated with ohm's formula $R=V \times I$, where R

(resistance, Ω) = I (current, Amps) x V (voltage, V) and TER ($\Omega \cdot \text{cm}^2$) = ($R_{\text{total}} - R_{\text{blank}}$) x SA where R_{total} is the resistance measured, R_{blank} is the resistance of the blank insert without any cells, and SA is the surface area of the inserts.

Experiments were performed after $R_{\text{Total}} > 1000$ ohms in order to ensure Calu-3 cell monolayers had indeed formed functional tight junctions. Values are reported as percentage decrease from the baseline values before treatments. Studies were performed in triplicate.

Gel Electrophoresis and Western blot analysis

To obtain total cell lysate the cells were washed three times in ice cold PBS and harvested with 100 μl of lysis buffer, freeze-thawed twice and scraped into microcentrifuge tubes. Lysis buffer was prepared using a base buffer containing 100mM NaCl, 20mM Tris-Cl pH 7.4, 1% Triton and 15% glycerol, supplemented with protease inhibitor cocktail (1:100, Calbiochem, Billerica, MA) and sodium orthovanadate (1:1000). Total cell lysates extracts were centrifuged at 13,000 rpm x for 20 min at 4⁰C. Total protein concentration in samples were measured at 450 nm using Pierce's BCA Protein Assay Reagent Kit, and using bovine serum albumin as standards, samples were read with an AD340 spectrophotometer and analysis software (Beckman Coulter, Brea, CA).

Protein samples were processed with 1:1 laemmli buffer complemented with 1:10 dichlorodiphenyltrichloroethane (DTT) and heated at 95°C for ten minutes. The proteins were separated using 12% SDS-PAGE in a Mini-Protean electrophoresis apparatus (BioRad, Waltham, MA). Each lane was loaded with

25 μ g of protein and 10 μ g of BioRad ladder 161-0318 was used for molecular weight identification. The gel was then transferred to a 0.45 μ m nitrocellulose membrane in a BioRad Western blot criterion cell. The membranes were then blocked overnight with 5% bovine serum albumin in PBST (PBS, 0.1% Tween 20) at 4 °C. I utilized either beta-actin or ponceau staining as a loading control by the method of Romero [43]. The appropriate primary antibody dilution of either: phosphorylated EGFR, phosphorylated ERK 1/2 (CellSignal), Occludin and ZO-1 (Zyomega) was added for 1 hour at room temperature. Secondary antibody GAx-HRP (BioRad) was added for 1 hour at room temperature. An amplification step was performed using a Blot Amplification module (BioRad). After amplification, colorimetric detection was performed using Opti-4CN Substrate Kit (BioRad) for 30 minutes. Immunoblots were documented using UVP GelDoc-IT imaging System (UVP, Upland, CA) and quantified with ImageJ software (NIH).

Immunofluorescence Microscopy

Confluent monolayers were seeded in 96-well tissue culture plates (CoStar, Corning, NY) or mounted on chambered slides systems (Lab-Tek, Rochester, NY) and treated according to the above procedures. After the experiments were completed, cells were washed three times with PBS and fixed with 3.7% paraformaldehyde in PBS for 10 minutes at room temperature. Cells were permeabilized with a 0.1% Triton-X 100 in PBS solution for 5 minutes. After washing twice with PBS, nonspecific binding sites were blocked with 1% bovine

serum albumin (BSA) for 30 minutes. Rinsed slides were incubated with Alexa Fluor 594 Phalloidin (Invitrogen, Camarillo, CA) in a 1% BSA solution in PBS for 20 minutes in the dark at room temperature for f-actin staining. Slides were washed twice with PBS and incubated at 37°C in the dark with FITC conjugated mouse anti-occludin (Zymed, Camarillo, CA) or FITC conjugated mouse anti-ZO-1 (Promega, Madison, WI) for 60 minutes at 37°C. Following two washes with PBS, I added a nuclear counterstain, DAPI (4',6'-di-amidino-2-phenylindole, Invitrogen, Camarillo, CA) for 5 minutes. The monolayers were examined under an Olympus fluorescent microscope equipped with an Olympus DP30BW digital camera (Olympus, Center Valley, PA). Photomicrography was performed under 600x and images were overlaid and pseudocolored (green –occludin, blue-actin) for ease of visualization.

Statistical Analysis

Statistical analysis of the differences between the means was performed with GraphPad Prism 6 (GraphPad Software, San Diego, CA). The results from TER and relevant band intensities are presented as mean \pm 95% confidence intervals, using either a paired or unpaired Student's *t*-test. Probability values ($p < 0.05$) were considered statistically significant.

Results

Pseudomonas elastase increases paracellular permeability on polarized Calu-3 cells

I grew polarized epithelia, by seeding Calu-3 cells in transwell permeable supports. After 8-10 days of incubation, visual inspection indicated that Calu-3 cells had formed monolayers. Comparison of TER before and after PE exposures indicated a time-dependent increase in paracellular permeability when apical domains of confluent monolayers were exposed to 2 U/ml of PE. Within 30 minutes, TER values had decreased by 15.53% and after 1 hour a 27.45% decrease in resistance was observed, which was significantly different compared to a loss of 0.76% ($t=3.072$, $df=4$, $p<0.001$), in control monolayers (Figure 2). After 2 hours of PE treatment, TER values had dropped to 61.27% ($t=3.142$, $df=4$, $p<0.001$) relative to control. My results indicate that PE induces tight junction disruption in a time-dependent manner.

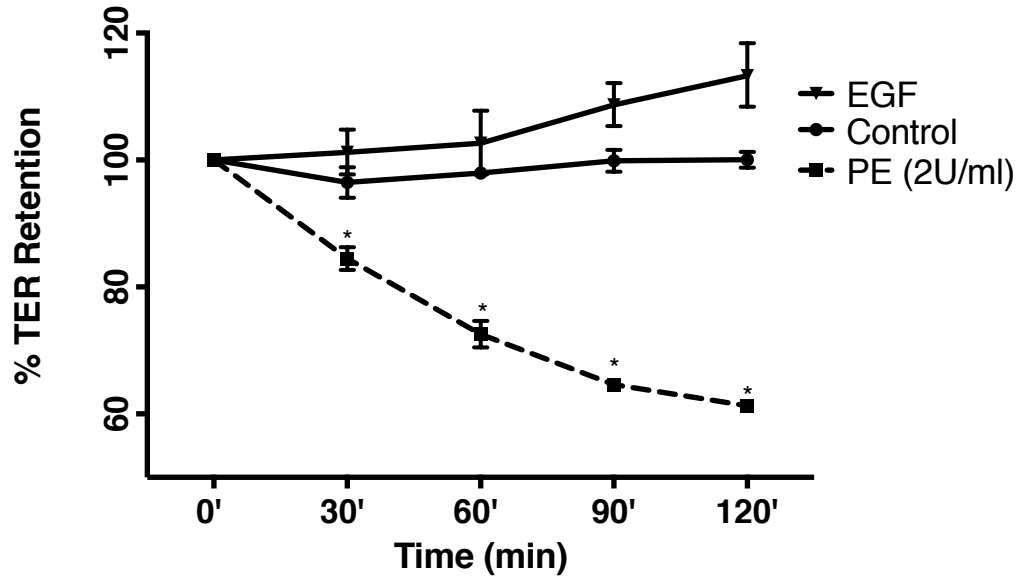


Figure 2. PE disrupts epithelial permeability as measured by TER. Calu-3 monolayers grown in transwell inserts showed a significant PE-induced decrease in electrical resistance across the cell membranes. Data presented as Mean \pm 95% CI of 4 independent experiments in triplicate wells. * indicates significant changes in TER at $p < 0.01$ compared with control

Epidermal growth factor receptor inhibition mitigates PE-induced disruption of epithelial permeability

To investigate whether PE utilizes epidermal growth factor receptor (EGFR) activation to alter paracellular permeability. For functional assays, the monolayers were pre-treated with AG1478, a specific EGFR tyrosine kinase inhibitor (EGFRi) for 30 minutes prior to PE exposure. After 30 minutes of PE exposure cells treated with EGFRi sustained their integrity- an insignificant 3.55% decrease in TER. After 1 hour a maximum TER loss of 7.47% was observed, which was statistically different ($t=3.007$, $df=4$, $p<0.05$) when compared to monolayers exposed to PE only (Figure 3). The subsequent TER decline in EGFRi + PE cells was gradual within the first 90 minutes of exposure, after which time TER stabilized.

Albeit, EGFRi did not completely prevent PE induced disruption, it did effectively help maintain high TER values. Overall, PE's disruptive effects saw an increase of 19.98% in TER when Calu-3 cells were pre-treated with EGFRi and then exposed to 1 hour of elastase. Although, I did observe a small but significant drop in TER in monolayers exposed to EGFRi alone, 10.65% ($t=3.159$, $df=4$, $p<0.05$) at the end of a 120-minute experiment. These results suggest that the observed PE induced increase in paracellular permeability is in part, dependent on activation of EGFR by elastase.

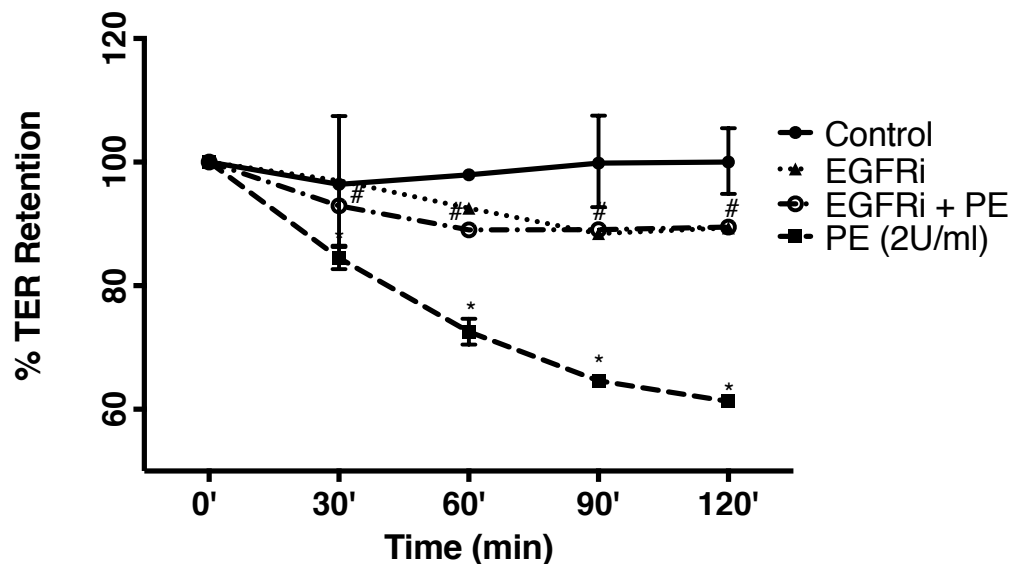


Figure 3. Effects of EGFR inhibition and PE exposure on tight junction integrity as measured by TER. Cells exposed with AG1478 (EGFRi) for 30 minutes prior to treatment with PE retained high paracellular permeability. TER was measured as Ωcm^2 and is evaluated as % retention compared to their pre-treatment resistance. SD bars on EGFRi+PE were removed for clarity. Data presented as Mean \pm 95% CI of 4 independent experiments in triplicate wells. * Indicates significant changes in TER at $p < 0.01$ compared with control, # indicates significant changes in TER $p < 0.05$ compared to PE.

Pseudomonas elastase activates the epidermal growth factor receptor

In an effort to understand the mechanism of action of PE on EGFR-dependent TER alteration, I next investigated the effect of PE on EGFR phosphorylation. Western blot analysis indicated an increase in tyrosine phosphorylation of EGFR within 5 minutes of apical exposure of elastase (Figure 4A). I chose this early time point because phosphorylation of EGFR peaks within the first 10 of stimulation [50], and because I wanted to capture early, PE-dependent signaling events. Densitometric analysis of the bands showed a significant increase (41.78 ± 12.44 %, $t=3.358$, $df=4$, $p<0.05$) in phosphorylation levels when Calu-3 cells were exposed to PE. Furthermore, this PE-induced increase in EGFR phosphorylation was 6% higher than the phosphorylation state achieved by EGF (Figure 4B).

The degree of inhibition achieved by EGFRi on PE-phosphorylation was 74.05%, which correlates with an attenuated decrease in permeability ($t=5.048$, $df=4$, $p<0.01$) measured by TER. This suggests that PE can activate downstream signaling pathways mediated by the activity of EGFR tyrosine kinase phosphorylation.

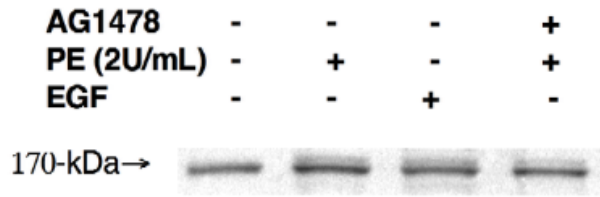


Figure 4A. PE phosphorylates Epidermal Growth Factor Receptor (EGFR Tyr-1068) within 5 minutes of apical exposure. Confluent Calu-3 monolayers were treated with 2U of active *Pseudomonas* elastase (PE) for 5 minutes. Representative western blot indicating EGFR activation was mitigated with a 30-minute pre-treatment of AG1478, (EGFR inhibitor). Experiments were run in triplicate.

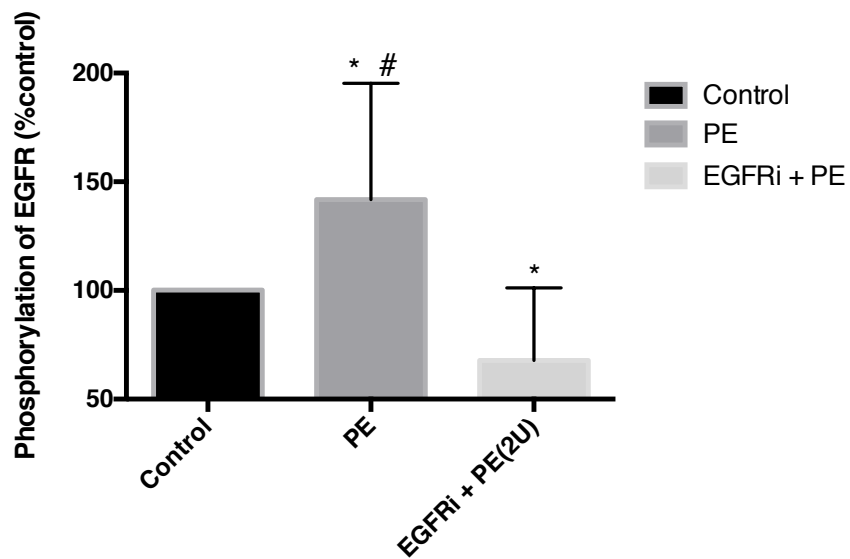


Figure 4B. Densitometric evaluation of phosphorylation of EGFR relative to control after exposure to 2 U/ml of PE. Densitometric analysis revealed a 35% increase in protein phosphorylation when Calu-3 cells were exposed to PE for 5 minutes. A tyrosine kinase inhibitor of EGFR (EGFRi) moderated activation of EGFR by PE. Data are reported as Mean \pm 95% CI. * P <0.05 versus control, # P <0.01, versus EGFRi + PE; n=4.

Role of EGFR in tight junctional proteins expression

Previous studies have shown that *Pseudomonas* elastase disrupts junctional proteins, including the scaffolding protein zonula occludens (ZO)-1 [10,24]. I sought to determine if PE renders its effects on TJ structure through activation of EGFR. I performed western blot analysis with monolayers after they had been exposed to 1-hour of PE, probing for total ZO-1 protein.

I detected bands in the 225-kDa regions corresponding to ZO-1 by western blotting. Exposure to 2 U/mL of PE for 1 hour significantly reduced ($t=17.44$, $df= 4$, $p<0.01$) ZO-1 protein expression levels by 52.86 ± 3.03 % (Figure 5B) relative to control which correlates, to TER levels of 72.55% in the same time period.

In monolayers pre-incubated with EGFRi, I was able to detect 75.10 ± 1.6 % of protein relative to control. This represents a conservation of 27.96 ± 3.43 % which is a significant ($t=8.136$, $df= 4$, $p<0.05$) conservation of ZO-1 protein expression during PE treatment (Figure 5B). This reduction in ZO-1 protein loss parallels maintenance of paracellular permeability since TER values at the same time point corresponded to readings of 89.01% compared to control.

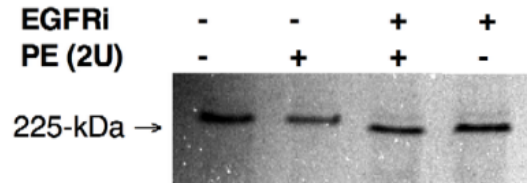


Figure 5A. Inhibition of EGFR decreased ZO-1 protein degradation after PE exposure. Representative western blot analysis after 1-hour exposure to PE using ZO-1 antibodies on Calu-3 monolayers. Cells maintained in serum free media (lane 1). A marked decrease in ZO-1 protein levels was observed on cells treated with PE alone (lane 2). Pre-incubating the monolayers with AG1478 diminished ZO-1 protein loss (lane 3). No change of ZO-1 expression was observed in cells treated with EGFRi alone (lane 4). Experiments were run in triplicate.

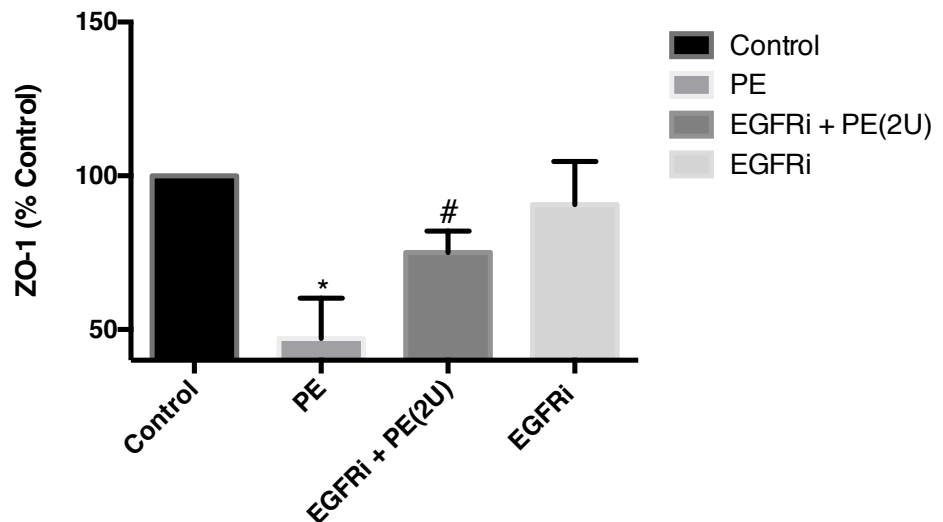


Figure 5B. Densitometric analysis of ZO-1 protein levels after exposure to PE, inhibition of EGFR diminished protein loss. Pre-treatment with an EGFRi maintained ZO-1 levels at 75.10% relative to control. Data are reported as mean \pm 95% CI, # depicts $P < 0.05$ in EGFRi vs PE, * depicts $P < 0.01$ in PE vs Control; $n = 4$

EGFR inhibition attenuates PE-induced ZO-1 delocalization

Since the function of ZO-1 is not only determined by its expression but also by its molecular arrangement, I studied the cellular architecture under immunofluorescent microscopy to look for any PE-mediated changes. Immunofluorescence micrographs of control Calu-3 cell monolayers showed a well-defined staining of ZO-1 proteins where it appears localized to the cellular periphery (Figure 6A). In treated cells the continuous ring of ZO-1 was replaced by punctate structures with little fluorescence with scattered fluorescent points located in the cellular periphery and the cytosol. In some areas complete loss of fluorescence was visualized, even with higher exposure times (Figure 6B). These results suggest that PE is capable of delocalizing and possibly destroying TJ proteins.

Immunofluorescent microscopy revealed that EGFRi preserved ZO-1 structure and localization, where it presented sharper and brighter bands. The photomicrographs suggest down-regulation of ZO-1 expression and its localization at the periphery of the cells is regulated, in part, by EGFR activation (Figure 6C).

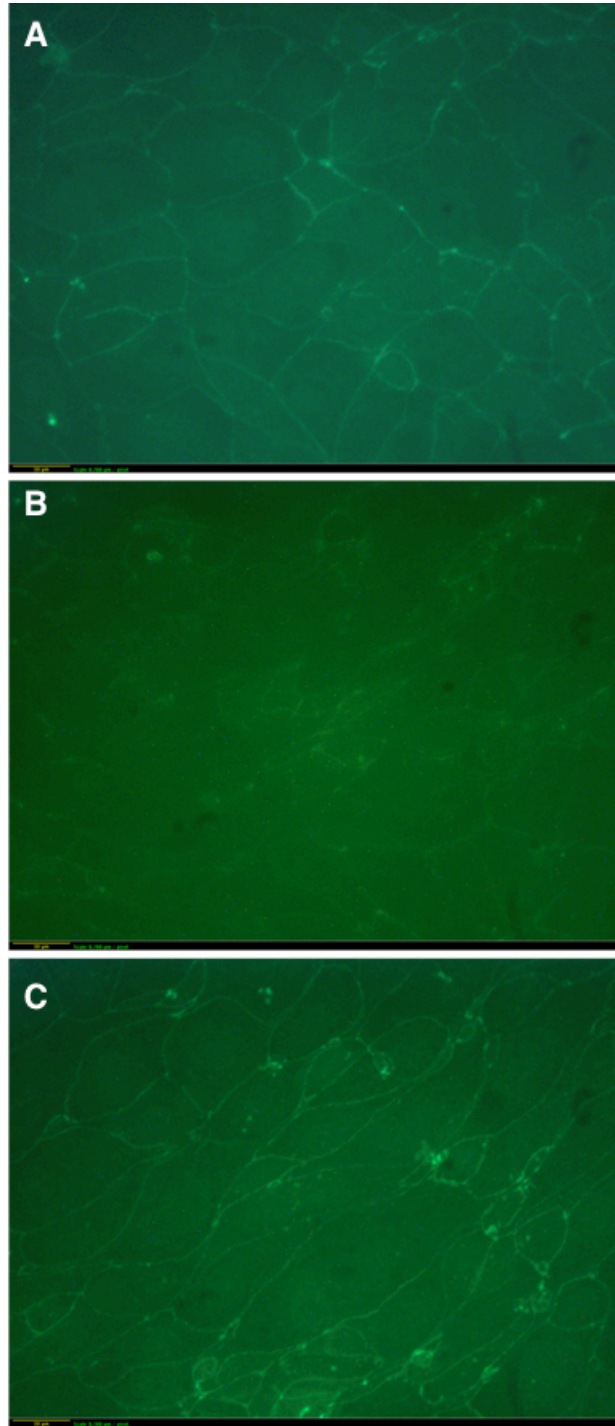



Figure 6. Immunofluorescence microscopy of tight junction protein ZO-1 of Calu-3 cells exposed to PE. Calu-3 cells were exposed apically to 2U of PE for 1 hour and incubated with FITC-conjugated mouse anti-ZO-1 post-treatment. **A.** Control. **B.** Cells exposed to PE only, exposure time had to be increased in order to visualize ZO-1. **C.** Calu-3 monolayers pre-incubated with AG1478 for 30 minutes prior to PE exposure. The results shown are representative of four independent experiments performed on slides in duplicate.  Scale bar 10 μ m

Inhibition of EGFR retains tight junctional protein occludin expression

I investigated whether high TER values obtained after 1 hour of PE application by inhibition of EGFR was related to expressional conservation of TJ protein occludin. I found a time-dependent depletion of occludin proteins in Calu-3 monolayers when exposed to PE (2U/mL) [18] (Figure 7A). Statistically significant changes were observed within 15 minutes of apical PE exposure, compared to control groups ($t=5.056$, $df= 4$, $p<0.01$). Within 30 minutes occludin expression in cells that had been treated with PE was $67.91 \pm 6.34\%$, and overall after 1 hour of PE, occludin had decreased by $72.85 \pm 5.39\%$, compared against control cells that were kept in serum free media.

Inhibition of EGFRi maintained relatively higher occludin levels. Within 15 minutes occludin was retained $29.79 \pm 11\%$ higher ($t=19.10$, $df= 4$, $p<0.05$), compared against cells that had been treated PE alone (Figure 7B). Occludin levels were preserved after 1 hour showing $85.94 \pm 3.77 \%$ expression, which suggests that PE induced occludin disruption, requires EGFR activation. Additionally, observational analysis of western blotting showed various bands or smudges (2 usually) around the 60-kDa mark in experiments that had been exposed to PE; thus indicative that perhaps PE changes occludin protein structure or its phosphorylation state.

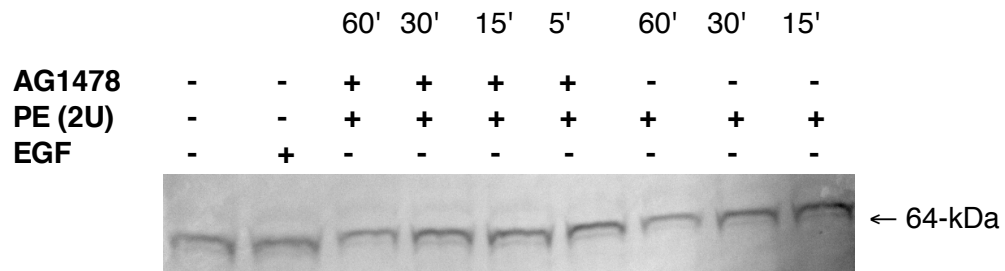


Figure 7A. EGFR inhibition prevents occludin translocation in a time-dependent manner. Representative immunoblot analysis with antibody against occludin showing confluent Calu-3 cells exposed to 2U of apical PE. Occludin protein levels decreased heavily after 30 minutes of PE exposure and rapidly afterwards. Inhibition of EGFR attenuated, but did not prevent complete occludin protein loss.

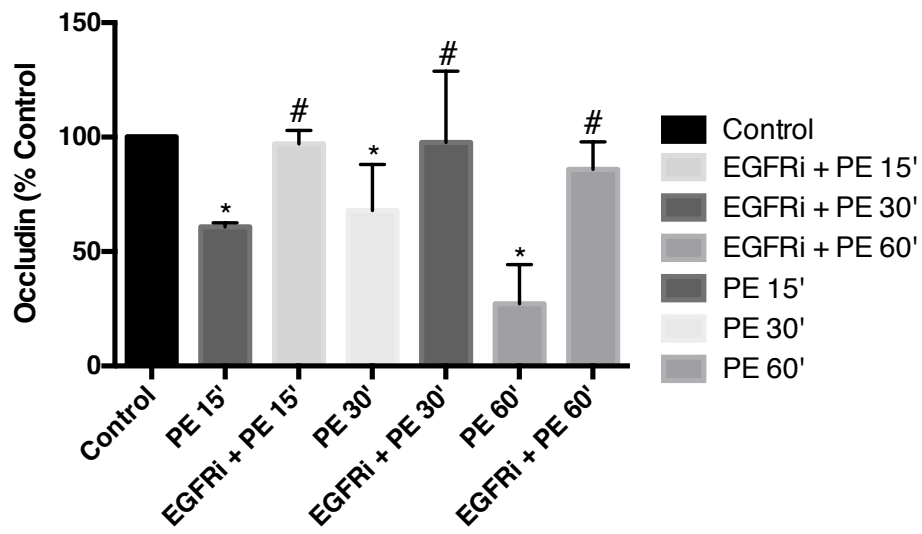


Figure 7B. EGFR inhibition sustained occludin protein levels after exposure to 2U of PE. Densitometric analysis of Calu-3 cells after apical exposure to 2U of PE at different time intervals. Inhibition of EGFR by AG1478 attenuated occludin protein loss in a time-dependent manner. After 60 minutes, occludin concentration was 56.15% higher in cells pre-incubated with EGFRi compared to cells treated with PE alone. Data are reported as Mean \pm 95% CI. # P <0.05 versus PE, * P <0.01, versus control; n=4.

PE induces translocation of occludin through EGFR activation

As with ZO-1, proper occludin function requires it to be accurately located on the cellular membrane. Immunofluorescence microscopy of Calu-3 monolayers revealed a strong affinity for FITC-labeled mouse anti-occludin antibodies. In control cells, occludin was seen aggregating around the periphery of the cellular membrane with continuous rings forming on the junctions with neighboring cells (Figure 8A).

I found PE translocated occludin from the cellular membrane and occludin diffusion was visualized as faint punctate rings. PE treated cells showed abnormal occludin staining, and revealed a complete loss of junctional rings formed by occludins of adjacent cells. Occludin morphology was also significantly altered, as normal occludin rings changed to undulate smeared structures (Figure 8B).

In cells that had undergone EGFR inhibition, retention of occludin staining and cell shape was visualized, which correlated with brighter immunofluorescence signals. In some cases, EGFRi treated slides showed that monolayers retained their junctional rings with neighboring cells (Figure 8C). Although, it is important to note that EGFRi did not completely prevent PE induced morphological occludin changes. In some cases punctation was present, indicative that some level of occludin translocation or diffusion had occurred. The results suggest that PE is able to modulate epithelial permeability by occludin translocation from the cellular periphery, in part by EGFR activation.

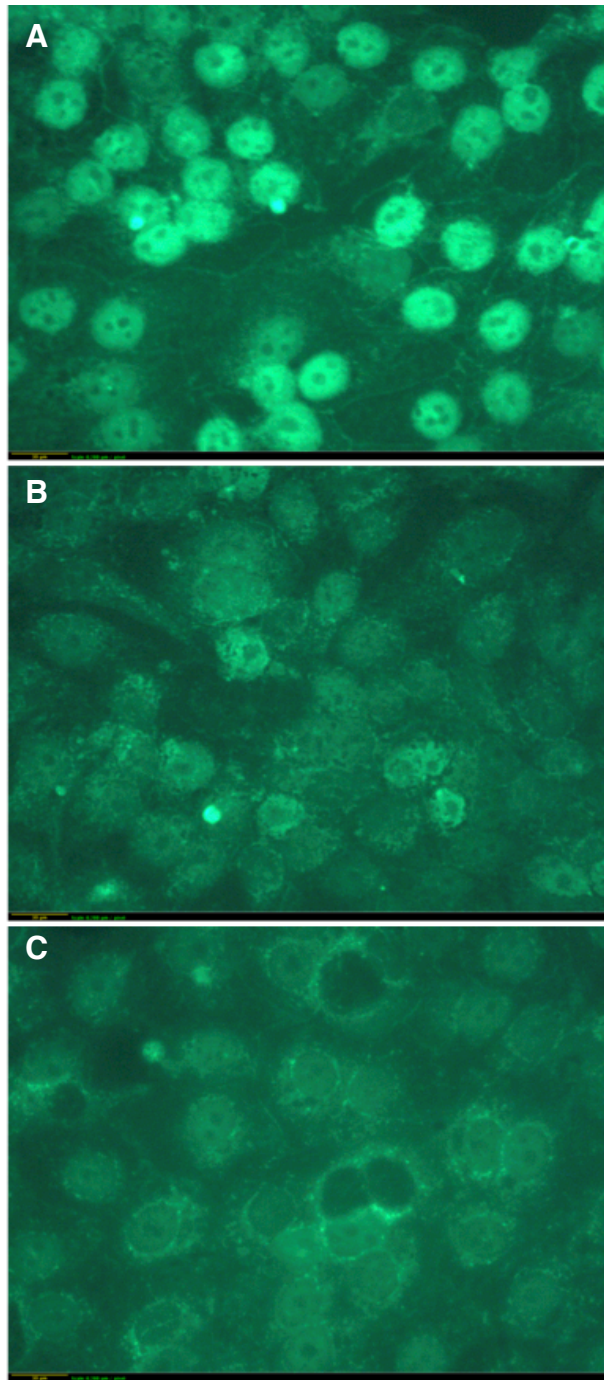



Figure 8. Immunofluorescence microscopy images of tight junction protein occludin exposed to PE. Monolayers were treated for 1 hour with 2U of apical PE and post-treatment were incubated with FITC-conjugated mouse anti-occludin. **A.** Control. **B.** Exposure to PE resulted in occludin delocalization and pigmentation. **C.** Pre-treatment with AG1478 maintained localization of occludin in monolayers and reduced disruption. The results shown are representative of four independent experiments performed on slides in duplicate.  Scale bar 10 μ m

PE disrupts occludin and ZO-1 colocalization with the cytoskeleton via an EGFR dependent mechanism

In order for epithelia to function as a defensive barrier, the tight junctions in the stratum corneum must work together. Tight junction function depends on the precise interaction between perijunctional proteins linking together with the actin cytoskeleton [12]. In order to assess if the interaction between ZO-1, occludin and the actin cytoskeleton is susceptible to morphological change induced by PE, I looked at fluorescent micrographs after fluorescent labeling using mouse monoclonal antibodies or Alexa Fluor Phalloidin staining of ZO-1, occludin and F-actin. Immunofluorescent images were then overlaid using ImageJ software.

In cells exposed to media only, I observed well defined staining of occludin, which appeared as a near continuous ring localized to the periphery of the cell (Figure 9A1). Filamentous actin appeared as numerous bands forming a ring-like structure that encircled the perijunctional area. Filaments were also dispersed among the cellular lumen (Figure 9A2). ZO-1 appeared as a bright ring localized to the cellular membrane (Figure 10A1), which interdigitated with F-actin in overlaid images (Figure 10A3). Overlaying occludin and F-actin micrographs revealed a number of areas with high cell-cell contact had reinforcing interactions between occludin and F-actin (Figure 9A3).

I detected distinct differences in monolayers that were exposed to PE; normal cellular morphology was lost in 1 hour, occludin (Figure 9B1) and F-actin both became disorganized and distorted (Figure 9B2). ZO-1 was delocalized

from the periphery and in some areas it appeared punctate and blurred (Figure 10B1). In areas that had highly distorted ZO-1, F-actin filaments were barely discernable and highly disrupted (Figure 10B2). In other experiments using brightfield illumination, cells exposed to PE detached from the extracellular matrix and became round and free floating, appearing as holes in the monolayer after immunofluorescence (Figure 9C1). PE was shown to cause severe disruption of the actin cytoskeleton. Results show a significant alteration in F-actin organization as well as reductions in staining intensity at the perijunctional ring (Figure 9B2). Interactions between occludin with F-actin were harder to visualize, in part due to changes in the arrangement of the actin cytoskeleton and occludin morphology (Figure 9B3).

Although inhibition of EGFR did not completely abolish PE-mediated effects on occludin and ZO-1 colocalization with F-actin, it attenuated the disruption and loss of colocalization between these proteins. F-actin staining appeared more prominent and sharp, with clear definition of the perijunctional ring (Figure 9C2, 10C2). Overlaying images with occludin and F-actin showed a higher degree of proximity than in monolayers treated with PE alone (Figure 9C3). Taken together, the data implies that PE induced occludin translocation, ZO-1 delocalization and F-actin disruption are in some part dependent on signaling stimulated by activation of EGFR.

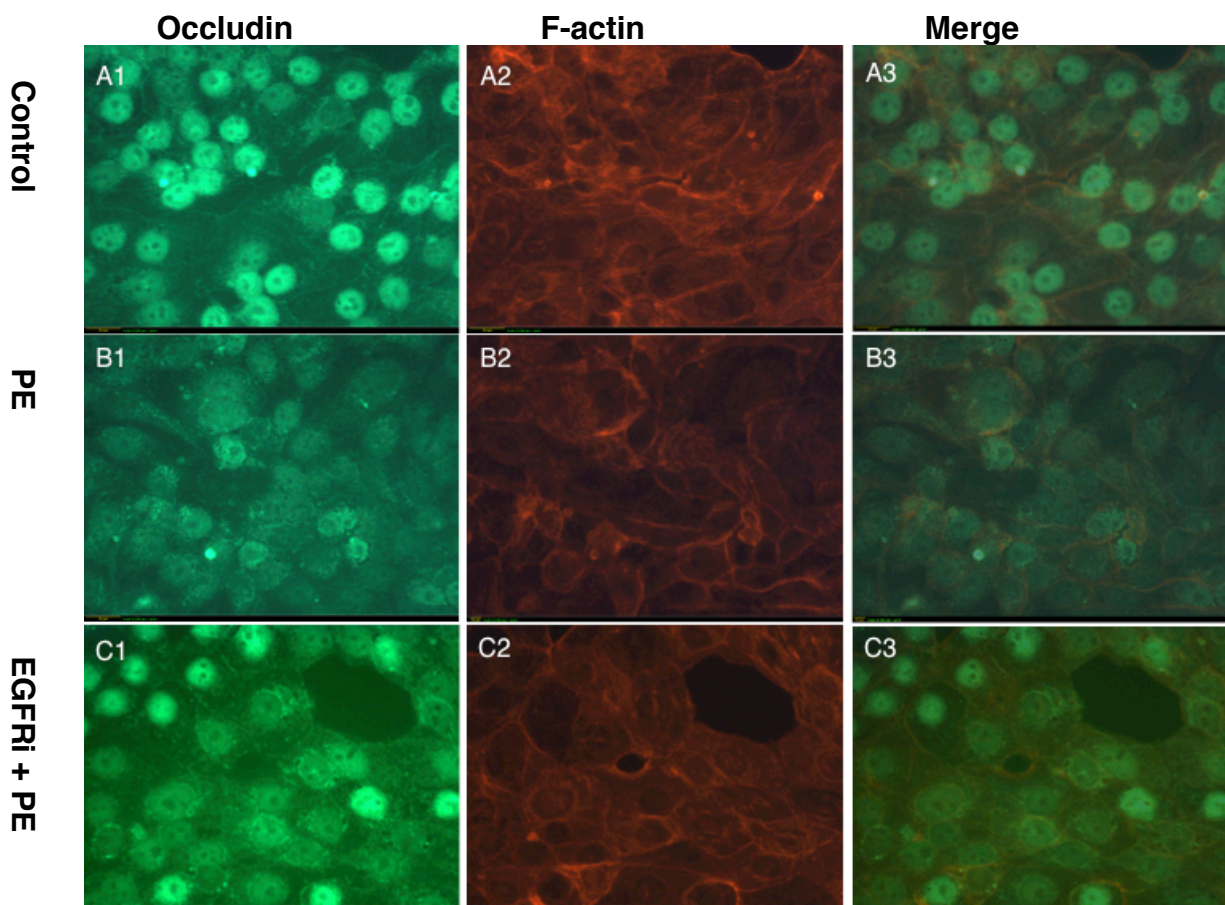



Figure 9. Representative photomicrographs of occludin and F-actin obtained by fluorescent microscopy after exposure to PE. Calu-3 cells were treated to 2U of PE for 1 hour, cells were then incubated with FITC conjugated anti-occludin (green) and Alexa 488 Phalloidin for F-actin (red). Overlaid images (last column) show marked decrease in colocalization of f-actin with occludin as well as loss of f-actin corresponding to changes in cellular morphology (middle column). The results shown are representative of four independent experiments performed on slides in duplicate.  Scale bar 10 μ m

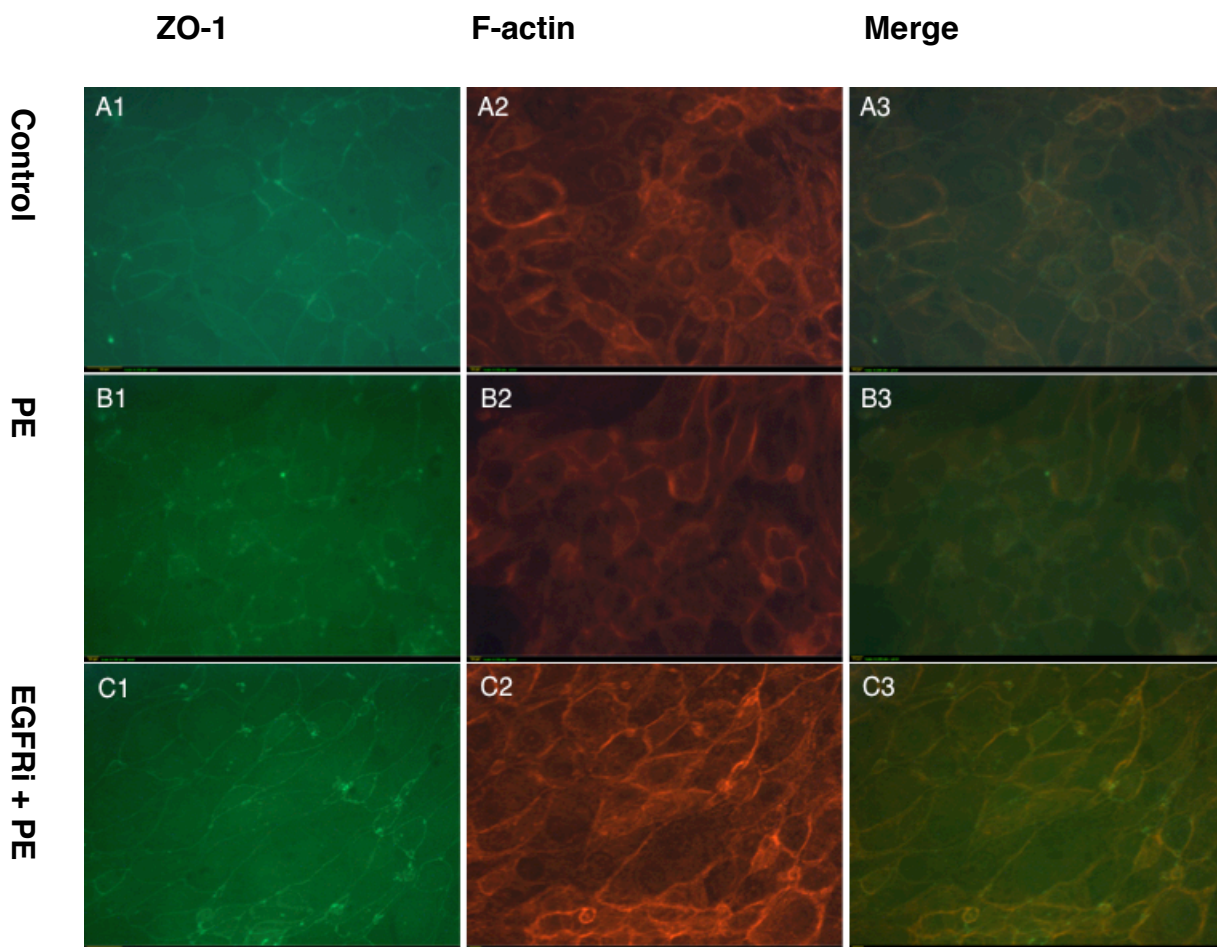



Figure 10. Representative photomicrographs of ZO-1 and F-actin obtained by immunofluorescence of Calu-3 cell monolayers after exposure to PE. Calu-3 cells were exposed apically to 2U of PE for 1 hour, after which they were fixed and stained with Alexa 488 Phalloidin selective for F-actin (red) and FITC labeled mouse anti-ZO-1 (green). A1-A3 control cells exposed to serum-free media. B1-B3, cells treated with PE show decline in F-actin and ZO-1 proteins as well as corresponding morphological changes. C1-C3, cells pre-treated with AG1478 show attenuated ZO-1 loss as well as diminishing F-actin protein disruption. The results shown are representative of four independent experiments performed on slides in duplicate.  Scale bar 10 μ m

Discussion

The pulmonary epithelium has evolved to function as a protective barrier against invasion by microorganisms and their metabolites. Tight junction formation between adjacent epithelial cells prevents passage of microbes and their toxins across the apical layer and into the basolateral domain [45]. Disruption of this protective barrier by bacterial elastase is a critical step in *Pseudomonas* infection [7] as it allows the bacterium to access the lung parenchyma and cause interstitial pneumonia and systemic infection and inflammation [13,46].

In this study, I utilized Calu-3 pulmonary epithelial cells as an *in vitro* model to determine what effects PE exposure has on barrier function and TJ structure. Calu-3 cells have a unique advantage provided by the fact that when they are grown in transwell inserts they form polarized monolayers containing tight junctions. Due to this cellular behavior, these cells have been used as a model of pulmonary epithelial barrier function [24,43,46].

The present study shows that PE mediates EGFR activation, which precedes changes in TJ structure and function. Western blotting indicates PE induced down-regulation of occludin and ZO-1 protein expression. A stark PE-mediated increase in paracellular permeability was associated with the disassembly of tight junctional proteins ZO-1, occludin and F-actin as observed via immunofluorescence microscopy and corresponding TER data.

The TER data implies that the destructive effects *Pseudomonas* elastase exerts on epithelial permeability are not just the consequences of elastolytic activity, but rather a combination of enzymatic and host signaling mechanisms that affect the epithelia in adverse ways. Maintaining high transepithelial electrical resistance by inhibiting EGFR during PE exposure, suggests that PE is capable of activation or transactivation of EGFR and downstream signaling mechanisms that lead to TJ disruption. Measured increases in paracellular permeability induced by PE, are in accordance with previous experiments performed with *Pseudomonas* elastase on polarized epithelial monolayers [10,24].

Interestingly, while inhibition of EGFR attenuated TER loss induced by PE, activation of EGFR by EGF slightly increased TER levels in a time-dependent manner. Suggesting that these two contrasting effects might be mediated by activation of different intracellular signaling pathways (Figure 1). Several studies show that polarized epithelia differ in the amount of EGF receptors found in the apical and basolateral domains and activation of these receptors lead to different downstream signaling pathways [53]. Normally the EGF receptor is predominantly localized to the basolateral surface in most epithelial cell lines[54-57], yet several hundred EGFR receptors per cell are located on the apical surface of epithelial cells [46,58]. Previous experiments had shown that TER values increase with exposure of exogenous apical EGF [59], and decreased with apical PE application [7,10,24], application of these molecules induced phosphorylation of EGFR. Densitometric analysis in my setup demonstrated that

PE was able to activate EGFR with marginally higher levels than human EGF indicating that differences measured were a result of either activation mechanisms of EGF receptors or antibody selection bias. For instance I noticed that PE has a higher affinity to 1068 than other tyrosine residues, whereas human EGF activates all tyrosine residues.

The differences observed in paracellular permeability could be caused by different downstream signaling mechanisms. A recent study, involving MAPK signaling using Calu-3 cells demonstrated for the first time that tight junctions in monolayers could be disrupted by cytokines [43]. Clark et al, have demonstrated that PE induces changes in PKC activation in Calu-3 cells. Increased PKC activation preceded TJ disruption through similar methods, loss of occludin and ZO-1 expression and localization. Clarke et al, also found that PE did not mediate these effects through proteolytic effects, since no discernable tight junctional proteins were found in the concentrated supernatant [24]. PKC-dependent pathways have been found to mediate TJ permeability induced by a variety of pathogens. One study found that *Helicobacter pylori* mediated activation of PKC, which led to TJ disruption [60]. Since several intracellular signaling pathways are influenced by both PKC and EGFR, it is possible that TJ disruption is induced by a combination of these effects [40,61,62]. In intestinal Caco-2 monolayers, inhibition of PKC activity attenuated TER increase induced by exogenous EGF application [63]. It is possible that cross-talk between EGFR and PKC signaling

may be an important mechanism used by *Pseudomonas* to mediate infection and invasion of pulmonary epithelia.

Tight junctional complexes are characterized by their junctional plasticity in terms of their quick ability to disassociate and reconstruct themselves, an essential process to normal cellular function [58]. Alteration of this process, however, may result in TJ disassembly and a subsequent increase in cellular permeability. The dramatic depletion (-72%) observed in western blots of TJ protein after 1 hour of PE exposure and the immunofluorescence observations revealing punctate structures replacing occludin suggest that TJ function should be compromised. However, a sharp drop in TER was not detected. It is likely that occludin disruption results in a limited amount of TER loss due to its partial regulatory role in tight junction function.

Recent reports indicate that occludin expression is not required in TJ formation in several epithelial tissue types including intestinal and sertoli cells [65,66]. Experiments with a mice gene-knockout model showed that claudin took over the role of occludin in TJ formation [67]. Another investigation suggested that occludin disruption does not induce claudin disturbance nor is it indicative of claudin protein loss [68]. In my study, I decided to disregard claudin expression or localization since previous results from our lab had determined that PE does not affect the fate of claudin.

I detected a loss of ZO-1 expression and found it dislocated from the cellular periphery. These deviations from normality were correlated with an

increase in paracellular permeability as measured by TER. ZO-1 functions as a scaffolding protein whose role is to link occludin to the actin cytoskeleton[18].

Even though filamentous actin is one of the most abundant proteins found in the cytoskeleton, its small size and resilience to degradation makes it difficult to measure small alterations. At present, one of the best techniques used to evaluate changes in F-actin is the highly specific, mushroom-derived toxin, phalloidin. This specific probe is useful because it recognizes filamentous actin but not free actin monomers [63]. Visualized filamentous F-actin provides insight into the fate of this protein during PE exposure.

Although intracellular signaling events can dictate function and localization of TJ proteins, they themselves must communicate in order to coordinate their structure. Occludin is normally found at high levels of phosphorylation at several serine and threonine residues. Conversely during disruption of tight junctions occludin primarily phosphorylate tyrosine residues in the C-terminal domain, which weakens its association with ZO-1[64,65]. Recently it was found that occludin tyrosine phosphorylation and disruption activates the extrinsic pathway of apoptosis in mammary (EpH4) epithelial cells [62,66]. Elastase may be capable of inducing similar effects through TJ signaling or by its mechanical disruption [67]

In conclusion, the results from this study indicate that *Pseudomonas* elastase is capable of quickly activating EGFR resulting in a novel mechanism through which it achieves increasing permeability in the pulmonary epithelium. As

for molecular mechanisms of this phenomenon, I noted that reductions in occludin and ZO-1 protein expression correlate with decreasing TER values. I observed occludin translocation from the cellular membrane, delocalization of ZO-1 from the cellular periphery and a high degree of cytoskeletal reorganization due to the mediation by PE-induced EGFR activation

References

1. Yu H, Hanes M, Chrisp CE, Boucher JC, Deretic V. (1998) Microbial pathogenesis in cystic fibrosis: pulmonary clearance of mucoid *Pseudomonas aeruginosa* and inflammation in a mouse model of repeated respiratory challenge. *Infection and Immunity* 66: 280-288.
2. Govan JRW, Deretic V. (1996) Microbial pathogenesis in cystic fibrosis: mucoid *Pseudomonas aeruginosa* and *Burkholderia cepacia*. *Microbiological Reviews* 60: 539.
3. Prince AS. (2002) Clinical implications of basic research: biofilms, antimicrobial resistance, and airway infection. *New England Journal of Medicine* 347: 1110-1111.
4. Costerton JW, Stewart PS, Greenberg EP. (1999) Bacterial biofilms: a common cause of persistent infections. *Science* 284: 1318-1322.
5. Tan MW, Rahme LG, Sternberg JA, Tompkins RG, Ausubel FM. (1999) *Pseudomonas aeruginosa* killing of *Caenorhabditis elegans* used to identify *P. aeruginosa* virulence factors. *Proceedings of the National Academy of Sciences* 96: 2408.
6. Mahajan-Miklos S, Tan MW, Rahme LG, Ausubel FM. (1999) Molecular mechanisms of bacterial virulence elucidated using a *Pseudomonas aeruginosa*–*Caenorhabditis elegans*. *Pathogenesis Model. Cell* 96: 47-56.
7. Azghani A, Connelly JC, Peterson B, Gray L, Collins M, et al. (1990) Effects of *Pseudomonas aeruginosa* elastase on alveolar epithelial permeability in guinea pigs. *Infection and Immunity* 58: 433.
8. Lee DG, Urbach JM, Wu G, Liberati NT, Feinbaum RL, et al. (2006) Genomic analysis reveals that *Pseudomonas aeruginosa* virulence is combinatorial. *Genome Biology* 7.
9. Robinson C. (1995) The airway epithelium: the origin and target of inflammatory airways disease and injury. *Immunopharmacology of the Respiratory System* London: Academic Press 187: 207.

10. Azghani AO. (1996) *Pseudomonas aeruginosa* and epithelial permeability: role of virulence factors elastase and exotoxin A. *American Journal of Respiratory Cell and Molecular Biology* 15: 132-140.
11. Friend DS, Gilula NB. (1972) Variations in tight and gap junctions in mammalian tissues. *Journal of Cell Biology* 53: 758-&.
12. Schneeberger EE, Lynch RD (2004) The tight junction: a multifunctional complex. *American Journal of Physiology-Cell Physiology* 286: C1213-C1228.
13. Lee A, Chow D, Haus B, Tseng W, Evans D, et al. (1999) Airway epithelial tight junctions and binding and cytotoxicity of *Pseudomonas aeruginosa*. *American Journal of Physiology Lung Cellular and Molecular Physiology* 277: L204-L217.
14. Rejman J, Di Gioia S, Bragonzi A, Conese M. (2007) *Pseudomonas aeruginosa* infection destroys the barrier function of lung epithelium and enhances polyplex-mediated transfection. *Human Gene Therapy* 18: 642-652.
15. Madden ME, Sarras MP. (1985) Development of an apical plasma-membrane domain and tight junctions during histogenesis of the mammalian pancreas. *Developmental Biology* 112: 427-442.
16. Godfrey RWA, Severs NJ, Jeffery PK. (1992) Freeze-Fracture morphology and quantification of human bronchial epithelial tight junctions. *American Journal of Respiratory Cell and Molecular Biology* 6: 453-458.
17. Gottardi CJ, Arpin M, Fanning AS, Louvard D. (1996) The junction-associated protein, zonula occludens-1, localizes to the nucleus before the maturation and during the remodeling of cell-cell contacts. *Proceedings of the National Academy of Sciences of the United States of America* 93: 10779-10784.
18. Stevenson BR, Siliciano JD, Mooseker MS, Goodenough DA. (1986) Identification of ZO-1: a high molecular weight polypeptide associated with the tight junction (zonula occludens) in a variety of epithelia. *The Journal of Cell Biology* 103: 755-766.

19. Fanning AS, Jameson BJ, Jesaitis LA, Anderson JM. (1998) The tight junction protein ZO-1 establishes a link between the transmembrane protein occludin and the actin cytoskeleton. *Journal of Biological Chemistry* 273: 29745.
20. Furuse M, Itoh M, Hirase T, Nagafuchi A, Yonemura S, et al. (1994) Direct association of occludin with ZO-1 and its possible involvement in the localization of occludin at tight junctions. *Journal of Cell Biology* 127: 1617-1626.
21. Furuse M, Hirase T, Itoh M, Nagafuchi A, Yonemura S, et al. (1993) Occludin: a novel integral membrane protein localizing at tight junctions. *The Journal of Cell Biology* 123: 1777-1788.
22. Wong V, Gumbiner BM. (1997) A synthetic peptide corresponding to the extracellular domain of occludin perturbs the tight junction permeability barrier. *The Journal of Cell Biology* 136: 399-409.
23. Morihara K, Tsuzuki H, Oka T, Inoue H, Ebata M. (1965) *Pseudomonas aeruginosa* elastase. *Journal of Biological Chemistry* 240: 3295.
24. Clark C, Thomas L, Azghani A. (2011) Inhibition of PKC attenuates *Pseudomonas aeruginosa* elastase-induced epithelial barrier disruption. *American Journal of Respiratory Cell and Molecular Biology*.
25. Azghani AO, Gray LD, Peterson BT, Johnson AR. (1991) Elastase from *Pseudomonas aeruginosa* alters integrity of intercellular junctions of cultured epithelial-cells. *Faseb Journal* 5: A1750-A1750.
26. Azghani AO, Baker JW, Shetty S, Miller EJ, Bhat GJ. (2002) *Pseudomonas aeruginosa* elastase stimulates ERK signaling pathway and enhances IL-8 production by alveolar epithelial cells in culture. *Inflammation Research* 51: 506-510.
27. Azghani A, Bedinghaus T, Klein R. (2000) Detection of elastase from *Pseudomonas aeruginosa* in sputum and its potential role in epithelial cell permeability. *Lung* 178: 181-189.

28. Wang Y, Zhang J, Yi X, Yu FSX (2004) Activation of ERK1/2 MAP kinase pathway induces tight junction disruption in human corneal epithelial cells. *Experimental Eye Research* 78: 125-136.
29. Miettinen PJ, Berger JE, Meneses J, Phung Y, Pedersen RA, et al. (1995) Epithelial immaturity and multiorgan failure in mice lacking epidermal growth factor receptor. *Nature* 376: 337-341.
30. Jorissen RN, Walker F, Pouliot N, Garrett TPJ, Ward CW, et al. (2003) Epidermal growth factor receptor: mechanisms of activation and signalling. *Experimental Cell Research* 284: 31-53.
31. Citri A, Yarden Y. (2006) EGF-ERBB signalling: towards the systems level. *Nature Reviews Molecular Cell Biology* 7: 505-516.
32. Gao JX, Li JL, Ma L. (2005) Regulation of EGF-induced ERK/MAPK activation and EGFR internalization by G protein-coupled receptor kinase 2. *Acta Biochimica Et Biophysica Sinica* 37: 525-531.
33. Wang YG, Du D, Fang LH, Yang G, Zhang CY, et al. (2006) Tyrosine phosphorylated Par3 regulates epithelial tight junction assembly promoted by EGFR signaling. *Embo Journal* 25: 5058-5070.
34. Raimondi F, Santoro P, Barone MV, Pappacoda S, Barretta ML, et al. (2008) Bile acids modulate tight junction structure and barrier function of Caco-2 monolayers via EGFR activation. *American Journal of Physiology-Gastrointestinal and Liver Physiology* 294: G906-G913.
35. Oda K, Matsuoka Y, Funahashi A, Kitano H. (2005) A comprehensive pathway map of epidermal growth factor receptor signaling. *Molecular Systems Biology* 1.
36. Petecchia L, Sabatini F, Usai C, Caci E, Varesio L, et al. (2012) Cytokines induce tight junction disassembly in airway cells via an EGFR-dependent MAPK/ERK1/2-pathway. *Laboratory Investigation* 92: 1140-1148.
37. Wan H, Winton H, Soeller C, Stewart G, Thompson P, et al. (2000) Tight junction properties of the immortalized human bronchial epithelial cell lines Calu-3 and 16HBE14o. *European Respiratory Journal* 15: 1058-1068.

38. Basuroy S, Seth A, Elias B, Naren AP, Rao R. (2006) MAPK interacts with occludin and mediates EGF-induced prevention of tight junction disruption by hydrogen peroxide. *Biochemical Journal* 393: 69-77.
39. Wretling B, Pavlovskis OR. (1983) *Pseudomonas aeruginosa* elastase and its role in *Pseudomonas* infections. *Reviews of Infectious Diseases* 5: S998-1004.
40. Azghani AO, Connelly JC, Peterson BT, Gray LD, Collins ML, et al. (1990) Effects of *Pseudomonas aeruginosa* elastase on alveolar epithelial permeability in guinea-pigs. *Infection and Immunity* 58: 433-438.
41. Olivera DS, Boggs SE, Beenhouwer C, Aden J, Knall C. (2007) Cellular mechanisms of mainstream cigarette smoke-induced lung epithelial tight junction permeability changes in vitro. *Inhalation Toxicology* 19: 13-22.
42. Crews CM, Alessandrini A, Erikson RL. (1992) The primary structure of MEK, a protein kinase that phosphorylates the ERK gene product. *Science* 258: 478-480.
43. Romero-Calvo I, Ocon B, Martinez-Moya P, Suarez MD, Zarzuelo A, et al. (2010) Reversible Ponceau staining as a loading control alternative to actin in Western blots. *Analytical Biochemistry* 401: 318-320.
44. Krall JA, Beyer EM, MacBeath G. (2011) High- and low affinity epidermal growth factor receptor ligand interactions activate distinct signaling pathways. *Plos One* 6.
45. Anderson JM, Van Itallie CM. (2009) Physiology and function of the tight junction. *Cold Spring Harbor Perspectives in Biology* 1.
46. Kipnis E, Sawa T, Wiener-Kronish J. (2006) Targeting mechanisms of *Pseudomonas aeruginosa* pathogenesis. *Medecine et maladies infectieuses* 36: 78-91.
47. Kuwada SK, Lund KA, Li XF, Cliften P, Amsler K, et al. (1998) Differential signaling and regulation of apical vs. basolateral EGFR in polarized epithelial cells. *American Journal of Physiology-Cell Physiology* 275: C1419-C1428.

48. Bishop WP, Wen JT. (1994) Regulation of Caco-2 cell proliferation by basolateral membrane epidermal growth factor receptors. *American Journal of Physiology-Gastrointestinal and Liver Physiology* 267: G892-G900.
49. Mori S, Morishita Y, Sakai K, Kurimoto S, Okamoto M, et al. (1987) Electron microscopic evidence for epidermal growth factor receptor (Egf-R)-like immunoreactivity associated with the basolateral surface of gastric parietal cells. *Acta Pathologica Japonica* 37: 1909-1917.
50. Playford RJ, Hanby AM, Gschmeissner S, Peiffer LP, Wright NA, et al. (1996) The epidermal growth factor receptor (EGF-R) is present on the basolateral, but not the apical, surface of enterocytes in the human gastrointestinal tract. *Gut* 39: 262-266.
51. Scheving LA, Shiurba RA, Nguyen TD, Gray GM. (1989) Epidermal growth factor receptor of the intestinal enterocyte - localization to laterobasal but not brush-border membrane. *Journal of Biological Chemistry* 264: 1735-1741.
52. Tong WM, Ellinger A, Sheinin Y, Cross HS. (1998) Epidermal growth factor receptor expression in primary cultured human colorectal carcinoma cells. *British Journal of Cancer* 77: 1792-1798.
53. Terakado M, Gon Y, Sekiyama A, Takeshita I, Kozu Y, et al. (2011) The Rac1/JNK pathway is critical for EGFR-dependent barrier formation in human airway epithelial cells. *American Journal of Physiology-Lung Cellular and Molecular Physiology* 300: L56-L63.
54. Terres AM, Pajares JM, Hopkins AM, Murphy A, Moran A, et al. (1998) *Helicobacter pylori* disrupts epithelial barrier function in a process inhibited by protein kinase C activators. *Infection and Immunity* 66: 2943-2950.
55. Xuan YT, Guo YR, Zhu YQ, Wang OL, Rokosh G, et al. (2005) Role of the protein kinase C Raf-1-MEK-1/2-p44/42 MAPK signaling cascade in the activation of signal transducers and activators of transcription 1 and 3 and induction of cyclooxygenase-2 after ischemic preconditioning. *Circulation* 112: 1971-1978.

56. Ping PP, Zhang J, Cao XN, Kong DY, Tang XL, et al. (1998) Brief episodes of ischemia induce activation of the MEK1/2-p44/p42 MAPK signaling cascade in the cytosolic fraction and subsequent nuclear translocation of p44/p42 MAPKs via a PKC-dependent pathway in conscious rabbits. *Circulation* 98: 586-586.
57. Suzuki T, Seth A, Rao R. (2012) Role of phospholipase C gamma-induced activation of protein kinase C epsilon (PKC epsilon) and PKC beta I in epidermal growth factor-mediated protection of tight junctions from acetaldehyde in Caco-2 cell monolayers (vol 283, pg 3574, 2008). *Journal of Biological Chemistry* 287: 6959-6959.
58. Funke L, Dakoji S, Bretz DS. (2005) Membrane-associated guanylate kinases regulate adhesion and plasticity at cell junctions. *Annual Review of Biochemistry* 74: 219-245.
59. Moroi S, Saitou M, Fujimoto K, Sakakibara A, Furuse M, et al. (1998) Occludin is concentrated at tight junctions of mouse/rat but not human guinea pig Sertoli cells in testes. *American Journal of Physiology-Cell Physiology* 274: C1708-C1717.
60. Al-Sadi R, Khatib K, Guo SH, Ye DM, Youssef M, et al. (2011) Occludin regulates macromolecule flux across the intestinal epithelial tight junction barrier. *American Journal of Physiology-Gastrointestinal and Liver Physiology* 300: G1054-G1064.
61. Saitou M, Furuse M, Sasaki H, Schulzke JD, Fromm M, et al. (2000) Complex phenotype of mice lacking occludin, a component of tight junction strands. *Molecular Biology of the Cell* 11: 4131-4142.
62. Beeman N, Webb PG, Baumgartner HK. (2012) Occludin is required for apoptosis when claudin-claudin interactions are disrupted. *Cell Death & Disease* 3.
63. Wulf E, Deboben A, Bautz FA, Faulstich H, Wieland T. (1979) Fluorescent phalloidin, a tool for the visualization of cellular actin. *Proceedings of the National Academy of Sciences of the United States of America* 76: 4498-4502.

64. Antonetti DA, Barber AJ, Hollinger LA, Wolpert EB, Gardner TW. (1999) Vascular endothelial growth factor induces rapid phosphorylation of tight junction proteins occludin and zonula occluden 1 - A potential mechanism for vascular permeability in diabetic retinopathy and tumors. *Journal of Biological Chemistry* 274: 23463-23467.
65. Rao R. (2009) Occludin phosphorylation in regulation of epithelial tight junctions. *Annals of the New York Academy of Sciences* 1165: 62-68.
66. Beeman NE, Baumgartner HK, Webb PG, Schaack JB, Neville MC. (2009) Disruption of occludin function in polarized epithelial cells activates the extrinsic pathway of apoptosis leading to cell extrusion without loss of transepithelial resistance. *Bmc Cell Biology* 10.
67. Rachow S, Zorn-Kruppa M, Ohnemus U, Kirschner N, Vidal-y-Sy S, et al. (2013) Occludin is involved in adhesion, apoptosis, differentiation and Ca²⁺ homeostasis of human keratinocytes: implications for tumorigenesis. *Plos One* 8.

Abstract

Pseudomonas aeruginosa Elastase Disruption of Tight Junctions via MAPK Signaling Pathway

Omar J. Castillo

Thesis Chair: Ali Azghani, Ph.D.

The University of Texas at Tyler
Spring 2013

Pseudomonas aeruginosa elastase (PE) is able to mediate pulmonary epithelial permeability, mainly by disrupting tight junction (TJ) function and structure. Previous studies have shown that PE induces several cellular responses including activation of protein kinase C (PKC) and the epidermal growth factor receptor (EGFR). The exact mechanism of epithelial disruption is not fully understood. The aim of this study was to determine if PE-induced TJ disruption was dependent upon activation of the extracellular signal-regulated kinases (ERK) arm of the mitogen-activated protein kinase (MAPK) pathway. I demonstrate that PE induces phosphorylation of ERK proteins within 5 minutes of apical exposure. Activation of MAPK preceded a loss of localization of TJ proteins occludin and zonula occludens (ZO)-1 and cytoskeletal reorganization. Furthermore, I propose that TJ disruption is elicited, in part, by activation of EGFR/MAPK signaling pathway by *Pseudomonas* elastase.

Chapter Two

Introduction

Pseudomonas aeruginosa is an opportunistic pathogen with a high intrinsic ability to resist common antibiotics [1]. This bacterium causes community acquired pneumonia and patients in critical care units frequently acquire *P. aeruginosa* induced ventilator-associated fatal pneumonia [2,3]. Furthermore, *P. aeruginosa* causes recurrent pulmonary infection in cystic fibrosis (CF) lungs, a common inherited disease among Caucasians [4,7]. In CF lungs, *P. aeruginosa* almost always mutates into a mucoidal strain, a phenotype that resists host immune systems and destruction by antibiotics [4-6]. Conversion to mucoid phenotype and formation of biofilm community in CF lungs enables *P. aeruginosa* to resist eradication and permanently colonize the lungs [8-10]. One of the initial putative destructive effects of *P. aeruginosa* is increased epithelial paracellular permeability, an event accomplished by disrupting tight junctions (TJ) [11,12]. Once multiprotein tight junctional complexes are disrupted, bacterial dissemination and potential systemic infection will follow [13]. An *in vitro* study using polarized cell monolayers indicated that cytotoxicity increased once *P. aeruginosa* gained access to the basolateral membrane [14]

Thus it is assumed that increased epithelial permeability accelerates morbidity and mortality of a *P. aeruginosa* pulmonary infection [1-5].

Several virulence factors and secreted proteolytic enzymes including elastase aid *P. aeruginosa* in disrupting TJs [5,15-18]. Pseudomonas elastase (PE) is a metalloprotease with a wide variety of effects, spanning from destruction of elastic tissue in the lungs, degradation of innate and adaptive immune components to initiating adverse host signaling pathways [12,15,19-22]. Bacteria lacking elastase are less virulent in acute as well as chronic models of pulmonary infection [13,23,24].

Previously I determined that *P. aeruginosa* elastase activates the epidermal growth factor receptor (EGFR) in Calu-3 monolayers. Activation of EGFR can have diverse results on TJ function [25-28]. Various secondary messenger systems are activated by EGFR, including the mitogen-activated protein kinase (MAPK) pathway, inositol trisphosphate (IP3) kinase pathway, Akt and the diacylglycerol (DAG) kinase pathway (Figure 1.) [25,29,30]. Azghani et al, reported that PE activates MAPK pathway intermediates in pulmonary fibroblasts and in primary rabbit alveolar type II cells [31]. Since various signaling pathways regulate the function and integrity of TJs, it is conceivable that PE utilizes specific intracellular host cells signals to modulate epithelial barrier function.

Activation of the MAPK signaling cascade is associated with transcription and translation of genes that are involved in the regulation of the cell cycle [32-34]. A significant body of evidence suggests that TJ disruption might occur through activation of the MAPK pathway in response to various stressors

[28,31,35]. In human colorectal epithelial cells (Caco-2) exposed to hydrogen peroxide, it was found that occludin, ZO-1 and their interactions with the actin cytoskeleton were mediated via MAPK signaling [36]. Activation of MAPK pathway mediated tight junction disassembly in 2 other bronchial epithelial cell lines, BEAS-2B and 16HBE14o, when they were exposed to cigarette smoke [37]. In Calu-3 monolayers cytokines induced tight junctions disruption by transactivation of EGFR and signaling through the extracellular signal-regulated kinase (ERK) 1/2 arm of MAPK pathway. The authors detected phosphorylated ERK levels within 5 minutes by western blot analysis and observation of TJ proteins with confocal microscopy showed that occludin and ZO-1 were no longer colocalized [28].

In an effort to dissect the signaling mechanisms by which PE induces TJ disruption, I looked at the signaling pathways activated by EGFR. Clark et al, demonstrated that PKC is activated in PE-mediated TJ disruption [21]. Another potential signaling pathway shared by EGFR/PKC is the MAPK signaling pathway[25]. The purpose of this study was to investigate whether increased epithelial permeability induced by elastase, requires activation of MAPK signaling cascade.

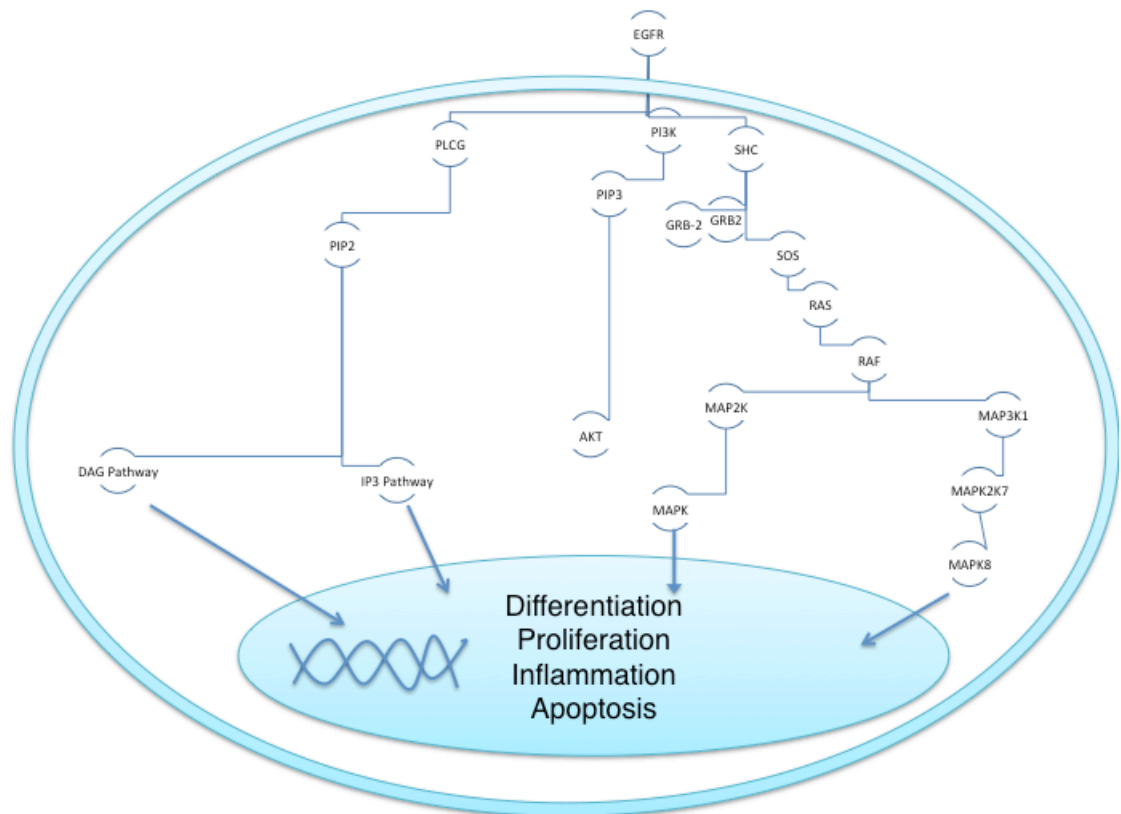


Figure 1. Schematic representation of several signaling pathways activated by the epidermal growth factor receptor [25]. Numerous signaling mechanisms are activated by phosphorylation of EGFR tyrosine kinase domains.

Materials and Methods

Cell culture

Human bronchial adenocarcinoma epithelial cell lines, Calu-3 (ATCC), were used as an *in vitro* model of epithelial cell injury. Calu-3 cells form tight junctions impermeable to ions and macromolecules [38,39]. Cells were cultured in RPMI-1640 (HyClone, South Logan, UT) and supplemented with 10% fetal bovine serum (Atlanta Biologicals, Lawrenceville, GA) and 1% L-glutamine (Cellgro, Herndon, VA). Cells were then incubated at 37 °C in an atmosphere of 5% CO₂ and maintained with a penicillin (100 U/ml) and streptomycin (0.1mg/ml) cocktail (BioWhittaker, Walkersville, MD). Cells were grown in 75cm² tissue culture flasks (Corning, Corning, NY) and were transferred at 80% confluency; all experiments were carried out between passage numbers 15-30. For epithelial permeability measurements, cells were seeded at a density of 1.0 x 10⁵ cells per insert, on a 6.5mm porous, polycarbonate tissue-culture transwell permeable insert (0.4 μm pore size and 0.33 cm², Costar, Lowell, MA) until they formed confluent monolayers. Before treatment, the cells were serum starved in RPMI-1640 with 1% L-glutamine for 12 hours.

Specific Inhibitors of Cell Signaling Pathways

To demonstrate the involvement of EGFR activation and signaling through an EGFR/MAPK signaling pathway, I utilized an EGFR tyrosine kinase inhibitor AG1478 (Calbiochem, La Jolla, CA). A MEK1/2 inhibitor U0126 (Calbiochem, La Jolla, CA) was used to block the activation of the extracellular signal-regulated

kinase (ERK1/2) arm of MAPK signaling pathway [40]. Cells were pre-treated for 30 minutes with either a 1 μ M dilution of AG1478 or a 25 μ M dilution of U0126, prior to being exposed to elastase. As a positive control I treated cells with epidermal growth factor (Sigma, St. Louis, MO) for 1 hour. All inhibitors were diluted in RPMI-1640 with 1% L-glutamine.

Bacterial Elastase

I utilized purified *P. aeruginosa* elastase (Elastin Product Co, Owensville, MO) to understand the cellular and molecular mechanisms involved in TJ disruption. Elastase applied it apically on Calu-3 monolayers at a concentration of 2 U/mL. On average a dose of 2 U/mL is found in the lungs of patients infected with *P. aeruginosa* based on antigen quantification from sputum samples [19]. Elastase had its purity and enzymatic activity confirmed using an elastin-fluorescein assay as recommended by the manufacturer.

Transepithelial Electrical Resistance

In order to quantitatively assess changes in paracellular permeability I measured changes in transepithelial electrical resistance (TER). Changes in TER were measured with chopstick-like electrodes placed in the apical and basal domains of confluent monolayers connected to a voltmeter (Millicell ERS, Billerica, MA). Readings were taken before and during apical treatment of the monolayers to evaluate their electrical resistance and tight junction integrity. Electrical resistance was calculated with ohm's formula $R=V \times I$, where R (resistance, Ω) = I (current, Amps) x V (voltage, V) and $TER (\Omega \cdot cm^2) = (R_{total} -$

$R_{\text{blank}} \times SA$ where R_{total} is the resistance measured, R_{blank} is the resistance of the blank insert without any cells, and SA is the surface area of the inserts.

Experiments were performed after $R_{\text{Total}} > 1000$ ohms in order to ensure Calu-3 cell monolayers had indeed formed functional tight junctions. Values are reported as percentage decrease from the baseline values before treatments. Studies were performed in triplicate.

Gel Electrophoresis and Western blot analysis

To obtain total cell lysate the cells were washed three times in ice cold PBS and harvested with 100 μl of lysis buffer, freeze-thawed twice and scraped into microcentrifuge tubes. Lysis buffer was prepared using a base buffer containing 100mM NaCl, 20mM Tris-Cl pH 7.4, 1% Triton and 15% glycerol, supplemented with protease inhibitor cocktail (1:100, Calbiochem, Billerica, MA) and sodium orthovanadate (1:1000). Total cell lysates extracts were centrifuged at 13,000 rpm x for 20 min at 4 $^{\circ}\text{C}$. Total protein concentration in samples were measured at 450 nm using Pierce's BCA Protein Assay Reagent Kit, and using bovine serum albumin as standards, samples were read with an AD340 spectrophotometer and analysis software (Beckman Coulter, Brea, CA).

Protein samples were processed with 1:1 Laemmli buffer complemented with 1:10 dichlorodiphenyltrichloroethane (DTT) and heated at 95 $^{\circ}\text{C}$ for ten minutes. The proteins were separated using 12% SDS-PAGE in a Mini-Protean electrophoresis apparatus (BioRad, Waltham, MA). Each lane was loaded with 25 μg of protein and 10 μg of BioRad ladder 161-0318 was used for molecular

weight identification. The gel was then transferred to a 0.45 μ m nitrocellulose membrane in a BioRad Western blot criterion cell. The membranes were then blocked overnight with 5% bovine serum albumin in PBST (PBS, 0.1% Tween 20) at 4 °C. I utilized either beta-actin or ponceau staining as a loading control by the method of Romero [41]. The appropriate primary antibody dilution of either: phosphorylated ERK 1/2 (CellSignal), Occludin and ZO-1 (Zyomega) was added for 1 hour at room temperature. Secondary antibody GAX-HRP (BioRad) was added for 1 hour at room temperature. An amplification step was performed using a Blot Amplification module (BioRad). After amplification, colorimetric detection was performed using Opti-4CN Substrate Kit (BioRad) for 30 minutes. Immunoblots were documented using UVP GelDoc-IT imaging System (UVP, Upland, CA) and quantified with ImageJ software (NIH).

Immunofluorescence Microscopy

Confluent monolayers were seeded in 96-well tissue culture plates (CoStar, Corning, NY) or mounted on chambered slides systems (Lab-Tek, Rochester, NY) and treated according to the above procedures. After the experiments were completed, the cells were washed three times with PBS and fixed with 3.7% paraformaldehyde in PBS for 10 minutes at room temperature. Cells were then permeabilized with 0.1% Triton-X 100 in PBS solution for 5 minutes. After washing twice with PBS, nonspecific binding sites were blocked with 1% bovine serum albumin (BSA) for 30 minutes. Rinsed slides were incubated with Alexa Fluor 594 Phalloidin (Invitrogen, Camarillo, CA) in a 1%

BSA solution in PBS for 20 minutes in the dark at room temperature for f-actin staining. Slides were then washed twice with PBS after which they were incubated at 37°C with FITC conjugated mouse anti-occludin (Zymed, Camarillo, CA) or FITC conjugated mouse anti-ZO-1 (Promega, Madison, WI) for 60 minutes at 37°C in the dark. Following two washes with PBS, I added a nuclear counterstain DAPI (4',6'-di-amidino-2-phenylindole, Invitrogen, Camarillo, CA) for 5 minutes and washed with PBS. The monolayers were examined under an Olympus fluorescent microscope equipped with an Olympus DP30BW digital camera (Olympus, Center Valley, PA). Photomicrography was performed under 600x and images were overlaid and pseudocolored (green –occludin, blue-actin) for ease of visualization.

Statistical Analysis

Statistical analysis of the differences between the means was performed with GraphPad Prism 6 (GraphPad Software, San Diego, CA). The results from TER and relevant band intensities are presented as mean \pm 95% confidence intervals, using either a paired or unpaired Student's *t*-test. Probability values ($p < 0.05$) were considered statistically significant.

Results

In vitro physiological assay displays Pseudomonas aeruginosa elastase induced increase in paracellular permeability

I measured PE induced changes on Calu-3 monolayers by measuring changes in transepithelial electrical resistance (TER). Exposing the model to 2 U/mL of PE showed a significant ($t=3.072$, $df= 4$, $p<0.01$) decrease of 15.53% in TER readings within 30 minutes. A substantial 27.45% loss in resistance was observed after 60 minutes, which was followed by a gradual but steady TER loss. After 2 hours TER had decreased by 38.73%, which was significant when compared to control wells in serum free media ($t=3.142$, $df= 4$, $p<0.001$) (Figure 2).

I sought to determine if PE engaged MAPK pathway activation as a mechanism to disruption epithelial integrity. I chemically inhibited MEK 1/2 with UO126 (ERKi) to prevent activation of ERK 1/2 proteins of MAPK pathway. Subsequent exposure of monolayers to PE did not alter their TER as the monolayers preserved over 90% of their TER values within the first hour of PE exposure. At 2 hours post PE-exposure, epithelial permeability readings were maintained at 83.51%, which was significantly ($t=3.38$, $df= 4$, $p<0.01$) higher than that of cells treated with PE alone (Figure 2). Quality assurance data indicated that application of ERKi had no adverse effects on TER in my model. Taken together, the results showed that PE induced TJ disruption is mainly dependent

on ERK 1/2 activation; and imply that MAPK signaling plays a role in homeostasis of the tight junction complex.

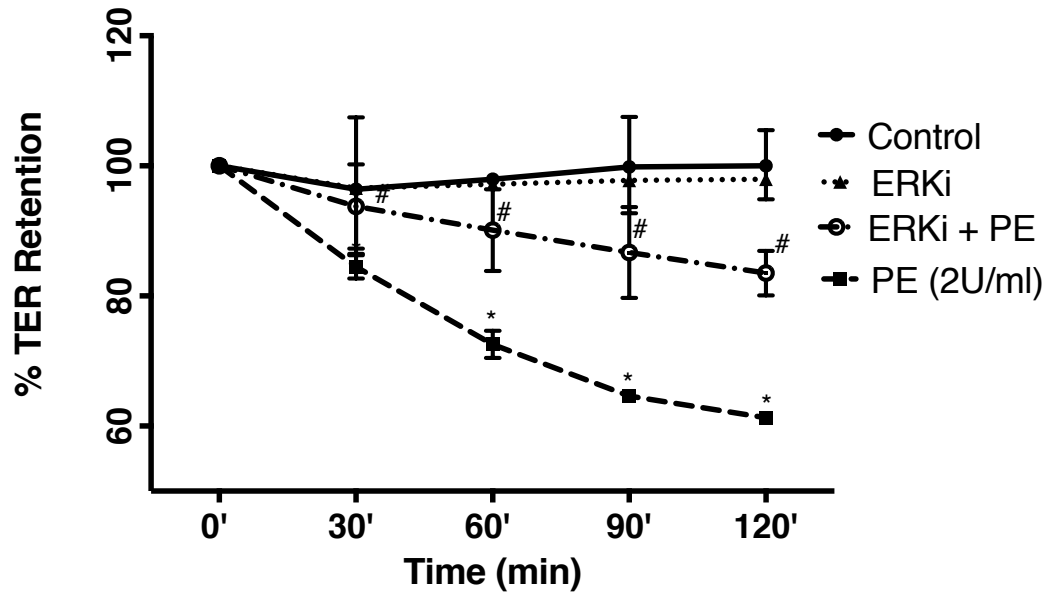


Figure 2. Inhibition of MAPK attenuated *Pseudomonas elastase* (PE) induced disruption of tight junction integrity as measured by TER. Calu-3 human lung cells cultured in permeable inserts. Cells pretreated with the specific kinase inhibitor (ERKi,U0126) for 30 minutes retained high paracellular permeability when exposed to PE. TER was measured as Ωcm^2 and is evaluated as % retention compared to their pre-treatment resistance values. Data presented as Mean \pm 95% CI of 3 independent experiments in triplicates, * $P < 0.01$ compared to control cells, # $P < 0.05$ compared to PE-treated monolayers.

Phosphorylation of the MAPK pathway by Pseudomonas elastase

Since inhibition of key proteins of the MAPK pathway preserved tight junctions function assessed by TER, I studied the phosphorylation status of ERK proteins in the MAPK pathway. Western blot analysis of ERK 1/2 indicated that PE induced phosphorylation of these proteins in serum-starved Calu-3 cells, within 5 minutes of apical application (Figure 3A). Densitometric analysis of the protein bands blotted onto the membrane revealed that PE enhanced phosphorylation of ERK 1/2, by $127.4 \pm 3.34\%$ ($t=8.114$, $df= 4$, $p<0.05$) relative to cells maintained in medium alone, as measured by densitometric analysis (Figure 3B). Inhibiting phosphorylation of ERK 1/2 with the MEK inhibitor U0126 prior to PE exposure, decreased the level of activated ERK 1/2 by decreased by $42.03 \pm 11.13\%$, ($t=3.77$, $df= 4$, $p<0.05$).

To clarify the relationship between EGFR activation and MAPK signaling induced by PE, I looked at expression levels of activated ERK 1/2 proteins of the MAPK signaling pathway in the presence of EGFR inhibitor AG1478 (EGFRi). In monolayers that had undergone EGFR inhibition prior to PE exposure I detected a $33.35 \pm 7.92\%$ decrease in expression of PE-induced phosphorylated ERK 1/2, ($t=4.21$, $df= 4$, $p<0.05$). These data indicate the PE activates the ERK intermediate protein of MAPK signaling pathway through receptors of epidermal growth factor.

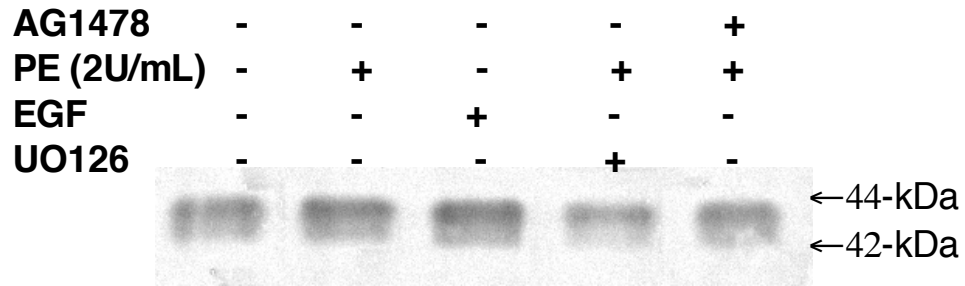


Figure 3A. Representative western blot analysis of confluent Calu-3 monolayers exposed for 5 minutes to 2 U/mL of PE. Activation of EGFR by PE, induces phosphorylation on Extracellular Signal-Regulated Kinases (ERK) 1/2 within 5 minutes. Pre-incubation with a MEK inhibitor (ERKi – U0126) or an EGFR inhibitor (AG1478) attenuated activation by PE.

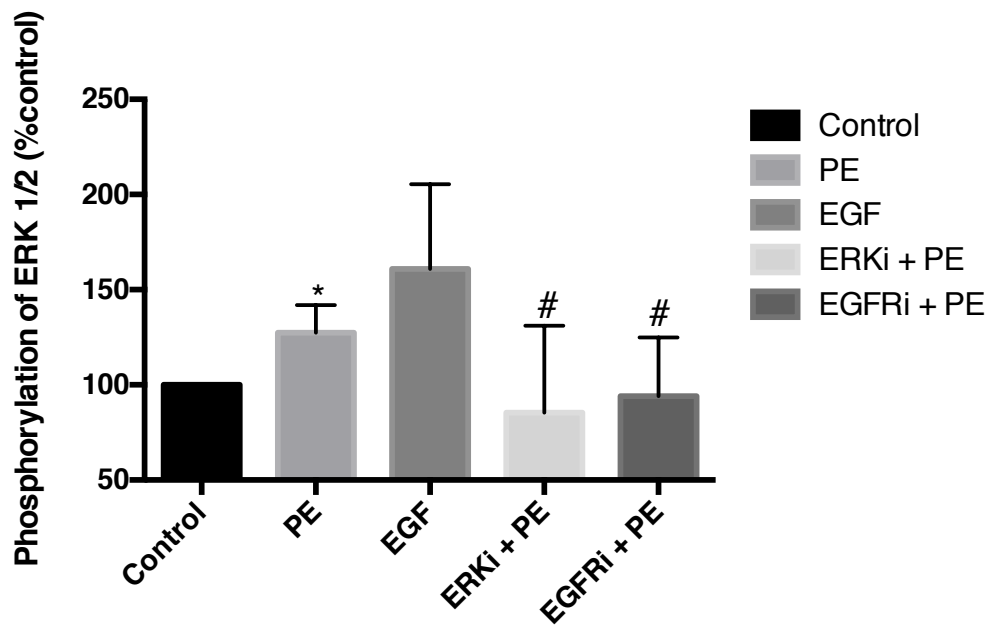


Figure 3B. Quantification of phosphorylation levels of ERK 1/2 protein in response to PE. Activation of the MAPK pathway occurred within 5 minutes of apical exposure to PE. Pre-incubation of Calu-3 cells with specific inhibitors of the EGFR or MAPK pathway (EGFRi and ERKi) attenuated the level of PE-induced ERK 1/2 phosphorylation. Data are reported as Mean \pm 95% CI. * P <0.05 compared with control, # P <0.05 compared with EGFR and MEK Inhibitor + PE.

PE-induced downregulation of ZO-1 expression is mediated by MAPK signaling

To understand the mechanism of PE induced ZO-1 disruption I studied the role of MAPK signaling in maintaining ZO-1 protein integrity. In cells pre-incubated with an ERKi, ZO-1 levels were maintained at $66.26 \pm 3.78\%$, which is on average a significant ($t=3.947$, $df=4$, $p<0.05$) increase of $19.13 \pm 4.84\%$ compared to cells treated with PE only (Figure 4B). Pre-treatment with ERKi was not significantly different from control, indicating the inhibitor had no adverse effect.

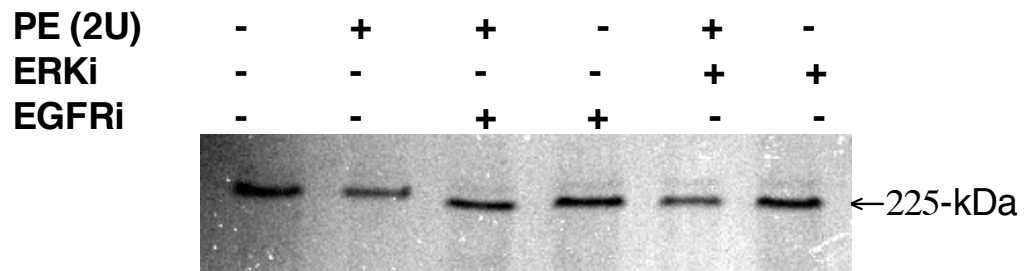


Figure 4A. Inhibition of EGFR and ERK decreased ZO-1 protein loss in Calu-3 cell lysates after PE exposure. Representative western blot analysis after 1-hour exposure to PE using ZO-1 antibodies on Calu-3 monolayers. A marked decrease in ZO-1 protein levels was observed on cells treated with PE alone. Pre-incubating the monolayers with AG1478 or U0126 diminished ZO-1 protein loss. Experiments were run in triplicate.

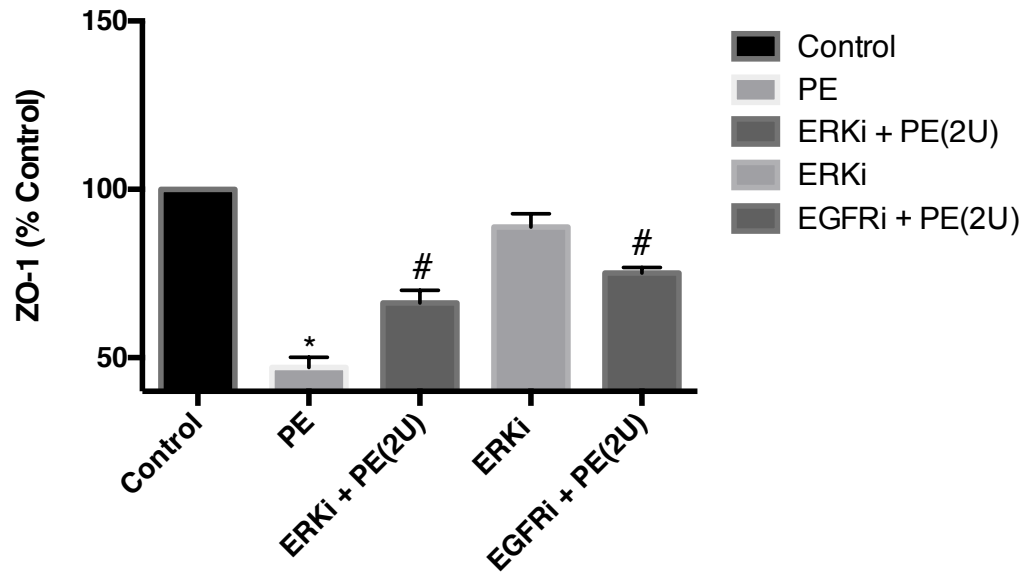


Figure 4B. Densitometry of ZO-1 protein expression after exposure to PE, inhibition of ERK diminished protein loss. Data are reported as mean \pm 95% CI # $P < 0.05$ inhibitors versus PE, * $P < 0.01$, PE versus Control; n=3

Inhibition of MAPK maintains localization of ZO-1 at the plasma membrane during PE exposure

Immunofluorescence microscopy was utilized to investigate effects of PE induced MAPK activation on ZO-1 localization and cell morphology.

Immunofluorescence micrographs probed with anti-ZO-1 antibodies revealed in control monolayers a distinct localization of ZO-1 protein assembly at the cellular periphery in control monolayers (Figure 5A). Fluorescence signal was strong and ZO-1 was easily distinguishable.

Loss of protein was observed as punctation of ZO-1 in cells treated with PE for 1 hour (Figure 5B). Some cell-cell contact areas showed complete loss of ZO-1 protein even with higher exposure times, a strong indicator of TJ disruption. PE-induced reduction in ZO-1 protein expression was attenuated by inhibition of

ERK 1/2 phosphorylation with U0126. A marked improvement in protein expression and localization in these cells was observed compared to cells treated with PE alone (Figure 5C). Inhibition of the MAPK activation diminished destructive effects of PE.

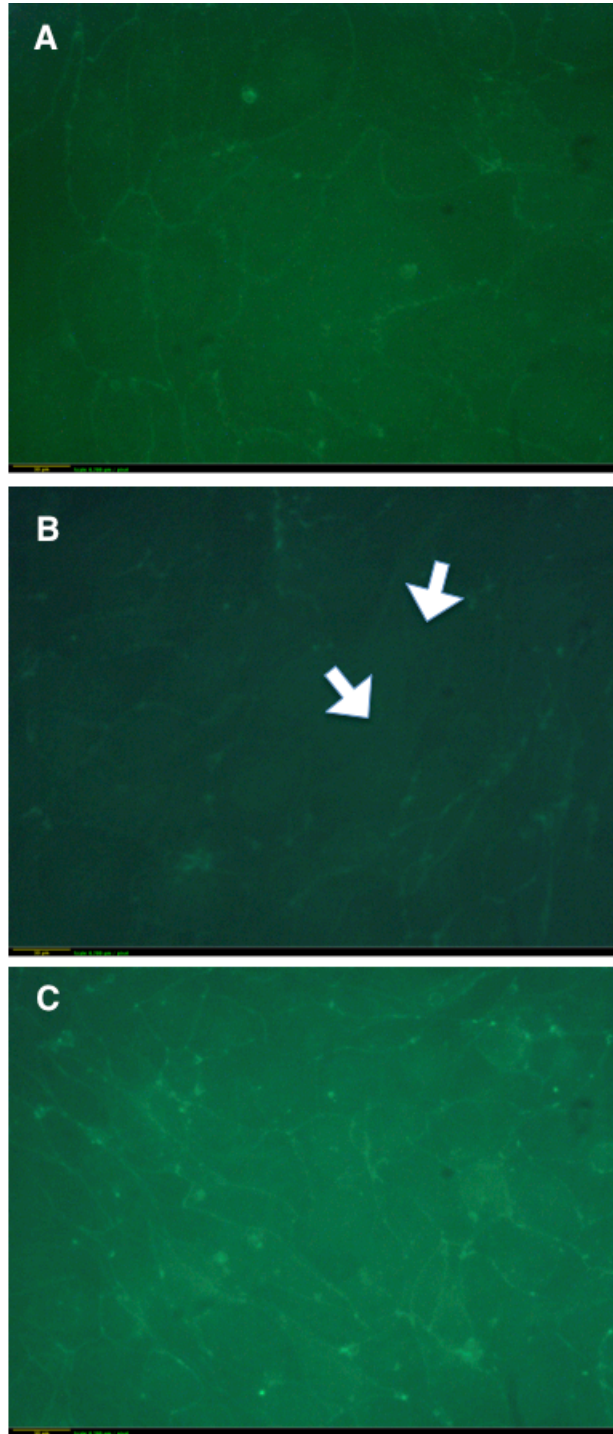



Figure 5. Immunofluorescence micrographs of tight junction protein ZO-1 of Calu-3 monolayers after exposure to PE (2 U/mL) for 1 hour. A. Control monolayers grown on chambered slides. **B.** PE treated cells arrows indicates areas where cell-cell contact was disrupted. **C.** Inhibition of MAPK by U0126 maintains ZO-1 protein expression and localization. The results shown are representative of three independent experiments performed in duplicates.  Scale bar 10 μ m. 600x.

PE mediated dislocation of occludin is dependent on MAPK signaling

I utilized FITC-conjugated mouse anti-occludin antibodies to determine the effects of PE on occludin expression and localization. In control chambers, occludin was localized to the cellular membrane where it formed continuous distinct rings at the junctions of adjacent cells (Figure 6A). I could neither detect disruptions in occludin nor observe any changes in cellular morphology under immunofluorescence or brightfield illumination. Treatment with PE for 1 hour showed alterations in occludin localization. This was observed as faint staining and smudged or indistinct occludin fluorescence throughout the membrane. Loss of protein in the membrane was also observed, as punctate structures replaced a continuous peripheral ring. Homotypic interactions with neighboring cells were lost and abnormal occludin morphology was prominent throughout the monolayer (Figure 6B).

Inhibition of the MAPK pathway significantly attenuated PE-induced disruption of occludin expression and organization (Figure 6C). Clearer staining with typical, spherical occludin distribution was observed. The junctional rings formed between adjacent cells were faint but still present. At times however, interspersed occludin was visualized through the cell membrane, indicating some degree of TJ disruption, which corresponds to decreased TER values.

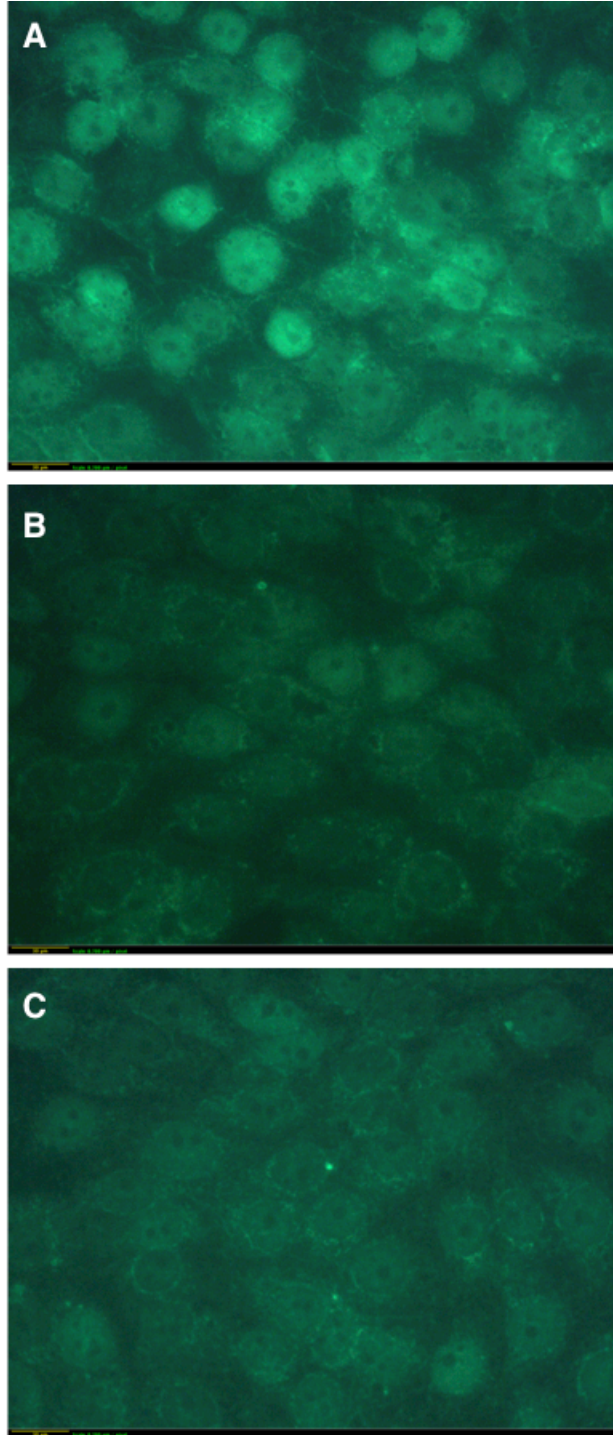



Figure 6. Immunofluorescence micrographs of tight junction protein occludin of Calu-3 cells exposed to elastase for 1 hour. A. Control monolayers cultured on chamber tissue culture slides **B.** Monolayers exposed to 2U/mL of PE. **C.** Cells pre-treated with U0126, a specific MEK inhibitor prior to PE. The results shown are representative of three independent experiments performed in duplicates.  Scale bar 10 μ m. 600x

PE decreases colocalization of occludin and ZO-1 with the actin cytoskeleton

A key defensive feature provided by TJs is the delicate balance of interdigitation between the cytoskeleton, ZO-1 and occludin [51]. In order to assess how MAPK-induced PE signaling disrupts TJs, I grew Calu-3 monolayers as described earlier, and stained F-actin fibers using Alexa Fluor 488 Phalloidin. In control cells the F-actin cytoskeleton was observed as a circumferential band around the cells with numerous filaments interdigitated within the cell membrane (Figure 7A2). The sharp immunofluorescence F-actin filaments were robust (Figure 8A2) and found to colocalize with both ZO-1 (Figure 8A3) and occludin rings (Figure 7A3). This event correlated with high levels of TER indicating increased tight junction function.

Taken together, I found ZO-1 (Figure 8B1) and F-actin (Figure 8B2) to be heavily distorted by PE in my *in vitro* model. A decrease in occludin fluorescence signal (Figure 7B1) indicated protein translocation from the cellular membrane; which showed atypical occludin and cytoskeletal disruption (Figure 7B2). In overlaid images a drastic reduction in colocalization between ZO-1 and the cytoskeleton was attributed to PE effects (Figure 8B3). In addition, there was little or no interaction between occludin and F-actin in PE-treated monolayers (Figure 7B3).

To determine if PE mediated these morphological changes through MAPK signaling, I pre-treated monolayers with an ERKi for 30 minutes prior to PE exposure. These cells exhibited retained F-actin staining (Figure 7C2). A high

degree of intracellular interdigitation of filamentous actin was also noticeable (Figure 8C2). Proximal localization of occludin with the cytoskeleton was clearer than in cells treated with PE alone (Figure 8C3). ZO-1 was found localized to the cellular periphery where it appeared to colocalize with F-actin. These data clearly indicate that PE mediates delocalization of TJ proteins through ERK 1/2.

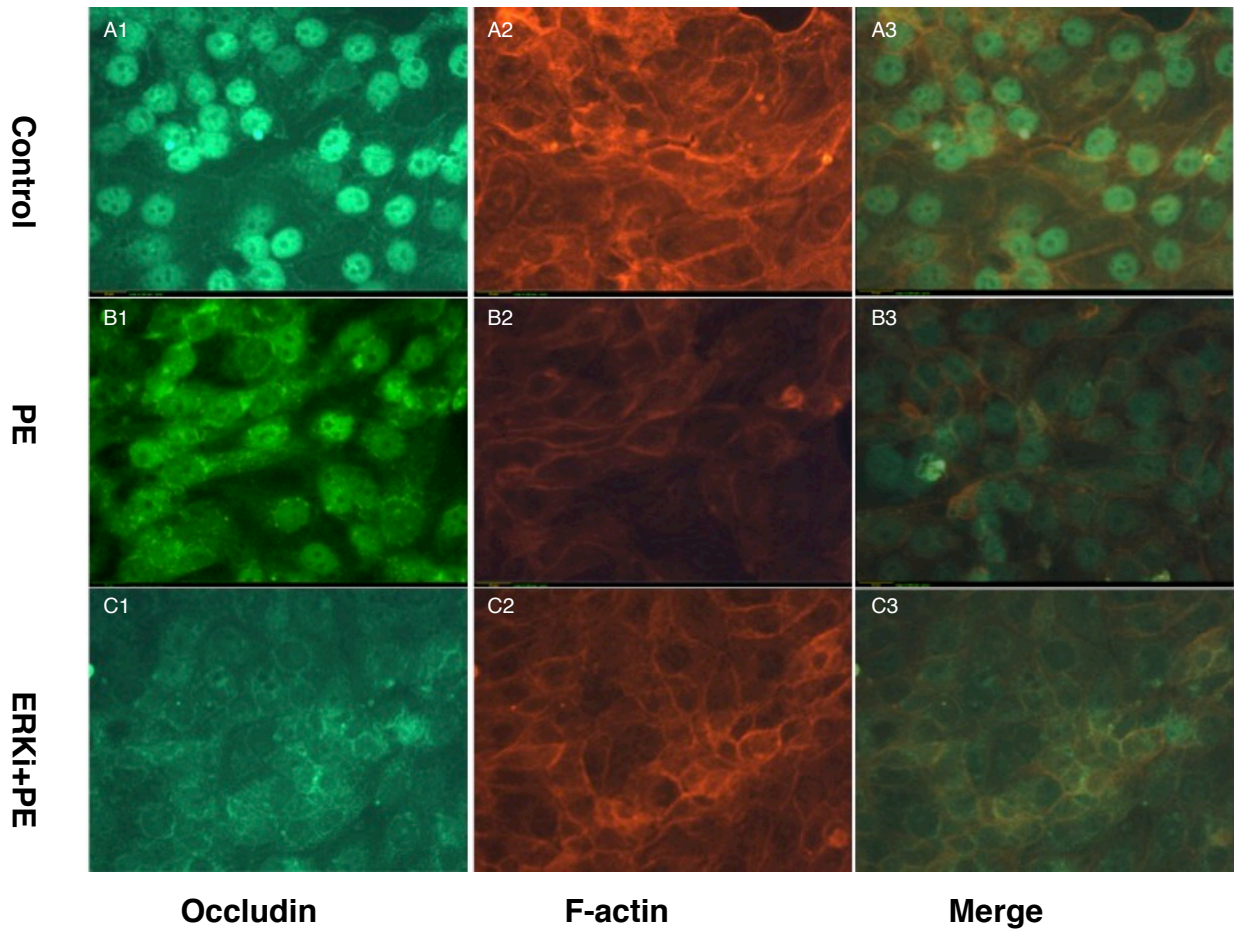


Figure 7. Representative micrographs obtained by immunofluorescence staining of occludin and F-actin. Green staining represents occludin, red staining represents F-actin and overlaid images of both occludin and F-actin are presented (last column). A1 – A3 control cells. B1-B3 cells exposed to 2U/mL of PE for 1 hour. C1-C3 PE exposure in ERKi pretreated cells. The results shown are representative of four independent experiments performed on slides in duplicate. Scale bar 10 μ m. 600x.

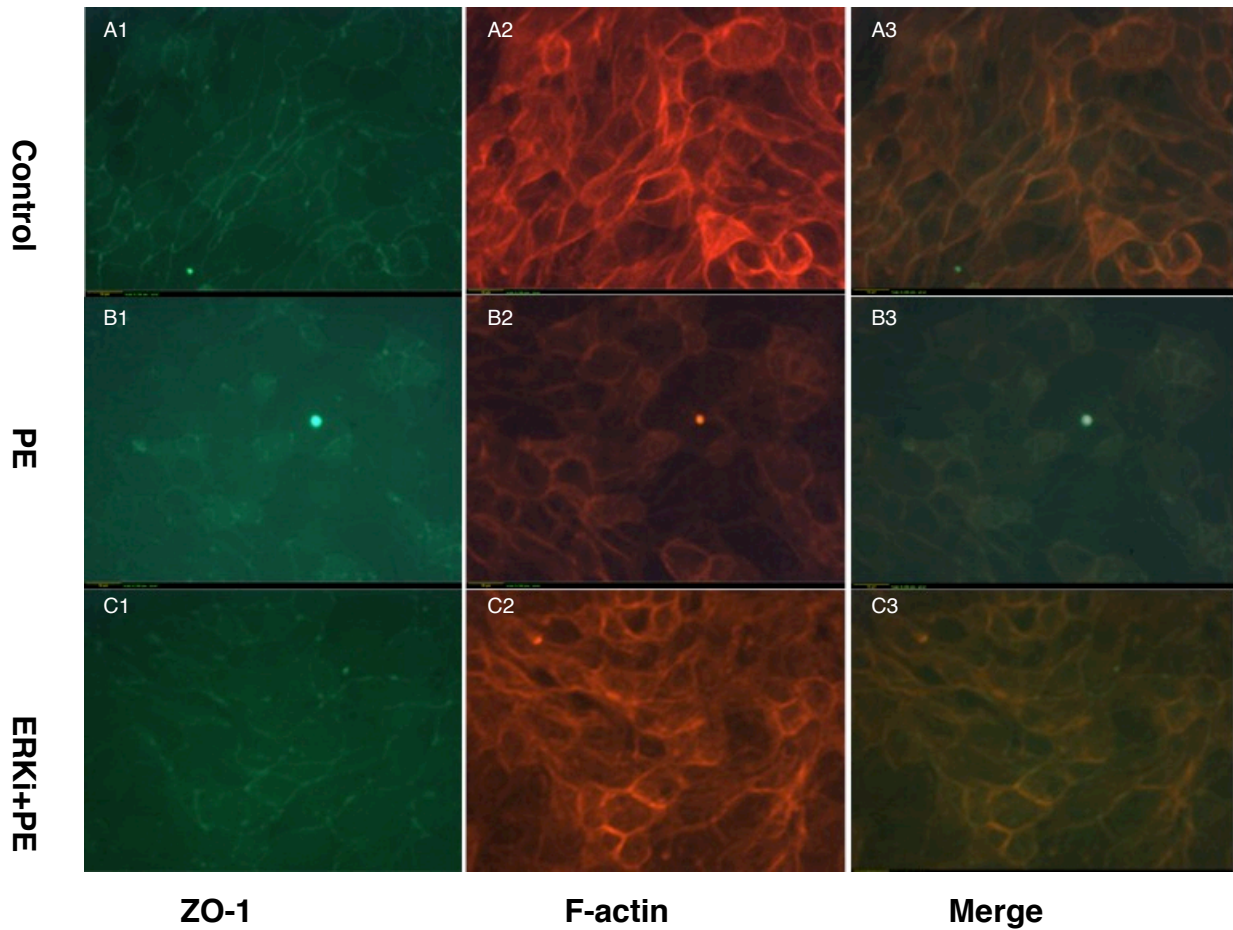


Figure 8. Representative fluorescent micrographs of ZO-1 and F-actin during PE exposure. Green staining represents ZO-1 (first column), red staining represents F-actin (middle column) and overlaid images of both ZO-1 and F-actin are presented in the last column. A1 – A3 control cells. B1-B3 cells exposed to 2U/mL of PE for 1 hour. C1-C3 PE exposure of ERKi pretreated cells. The results shown are representative of four independent experiments performed on slides in duplicate. Scale bar 10 μ m. 600x.

Discussion

The present study shows that *Pseudomonas* elastase is capable of activating mitogen-activated protein kinase (MAPK) signaling pathway. Activation of this pathway was associated with increased paracellular permeability as measured by changes in TER. Alterations in localization and interactions of TJ proteins ZO-1, occludin and F-actin were mediated by a PE-induced MAPK signaling mechanism. Furthermore I found that ERK 1/2 phosphorylation coincides with EGFR activation, suggesting the involvement of PE-induced EGFR/MAPK signaling pathways in TJ disruption.

Activation of MAPK has been associated with cell cycle events, which includes mitosis, differentiation, motility and gene expression as well as cellular apoptosis. Recently several studies have found that tight junctions are intimately associated with MAPK signaling [28,36,37,44-47]. One study with bronchial epithelial cell lines established that cigarette smoke induces ZO-1 delocalization by ERK 1/2 activation [37]. Knockdown of ERK by siRNA enhanced tight junction integrity and accelerated monolayer formation in undifferentiated epithelial colorectal cells [44]. When corneal epithelial cells were exposed to phorbol 12-myristate 13-acetate (PMA), tight junction disruption occurred via activation of ERK, an effect that was attenuated by pretreating monolayers with an inhibitor of MAPK signaling [48]. Studies with two cell lines of different origin (bronchial Calu-3 and intestinal Caco-2 monolayers) indicated that TJ disruption is mediated by EGFR induced MAPK activation when they were exposed to cytokines and bile

acids, respectively [26,28].

Our lab has shown that PE is capable of mediating MAPK activation in pulmonary fibroblasts (IMR90) and in primary alveolar type II epithelial cells. In both studies, MAPK activation was associated with an increase production of interleukin-8 (IL-8), a hallmark of pulmonary inflammation [31]. Increased IL-8 levels have also been associated with changes in TJ structure [28]. In intestinal epithelial cells (T-84), *Campylobacter jejuni* activates ERK phosphorylation and induces IL-8 secretion to the basolateral domain. The authors indicated that these events may contribute to TJ disruption [49]. In terms of PE-induced signaling and epithelial permeability, Clark et al indicated that PKC activation precedes destructive effects on the pulmonary epithelium [21]. PKC has been shown to strongly regulate TJ assembly and mediate the correct localization of several zonula occludens junctional proteins [50]. In support of my findings, several PKC isoforms have been shown to modulate ERK activity and produce changes in TJs induced by mediators other than PE [51-53].

A recent study demonstrated that inhibition of EGFR modulates activation of the MAPK pathway by cytokines in polarized epithelial monolayers, ERK moderated the fate of TJ proteins [28]. It is therefore plausible, that PE mediates TJ disassociation by a similar EGFR/MAPK signaling mechanism. Visual comparison between ERK and EGFR inhibited monolayers indicate that EGFRi cells retained more junctional proteins and the F-actin cytoskeleton presented increased interdigitation with both ZO-1 and occludin proteins during PE

exposure. This suggests that perhaps EGFR activation by PE is inducing signaling through multiple pathways that aid *Pseudomonas* in its pathogenesis. Additionally, my results demonstrate ERK activation is not completely dependent on EGFR phosphorylation, implying that other signaling mechanisms are involved in mediating PE-induced ERK 1/2 phosphorylation. It is conceivable that such signaling pathways as nuclear-factor kappa B, PKC, DAG and Akt may participate in PE-induced increases in paracellular epithelial permeability.

Taken together, I report that EGFR phosphorylation by PE induces ERK 1/2 activation. Monolayers that had undergone pre-treatment with an ERKi (U0126) retained TER after 1 hour of PE exposure. This observation is partly attributed to conservation of occludin and ZO-1 localization as visualized by immunofluorescence microscopy. In ERKi treated cells, the ZO-1 perijunctional ring showed successful colocalization with the actin cytoskeleton and unlike PE treated cells, occludin was not translocated from the cellular membrane as it occurred in PE treated cells. On occasion, however, occludin was visualized as punctate circular structures in ERK inhibited, PE treated monolayers. My results clearly indicate *P. aeruginosa* elastase mediates tight junctional changes through EGFR/MAPK signaling pathways.

Future research includes investigations to determine whether *Pseudomonas* elastase initiates occludin phosphorylation and mediates tight junction protein signaling; activation of occludin regulates tight junction structure and apoptosis. Additionally, we would like to discover the crosstalk between PE-

induced host signaling pathways and their role in pathogenesis of *Pseudomonas aeruginosa* in an effort to combat this devastating human pathogen.

References

1. Lyczak JB, Cannon CL, Pier GB. (2000) Establishment of *Pseudomonas aeruginosa* infection: lessons from a versatile opportunist. *Microbes and Infection* 2: 1051-1060.
2. Trouillet JL, Vuagnat A, Combes A, Kassis N, Chastre J, et al. (2002) *Pseudomonas aeruginosa* ventilator-associated pneumonia: comparison of episodes due to piperacillin-resistant versus piperacillin-susceptible organisms. *Clinical Infectious Diseases* 34: 1047-1054.
3. Spencer RC. (1996) Predominant pathogens found in the European prevalence of infection in intensive care study. *European Journal of Clinical Microbiology & Infectious Diseases* 15: 281-285.
4. Oliver A, Cantón R, Campo P, Baquero F, Blázquez J. (2000) High frequency of hypermutable *Pseudomonas aeruginosa* in cystic fibrosis lung infection. *Science* 288: 1251-1253.
5. Fantuzzi G, Wieland CW, Siegmund B, Vasil M, Senaldi G. (2001) Pulmonary inflammation induced by *Pseudomonas aeruginosa* virulence factors: role of IRF-1. *Journal of Leukocyte Biology*: 99-99.
6. Lee B, Schjerling CK, Kirkby N, Hoffmann N, Borup R, et al. (2011) Mucoid *Pseudomonas aeruginosa* isolates maintain the biofilm formation capacity and the gene expression profiles during the chronic lung infection of CF patients. *Apmis* 119: 263-274.
7. Macia MD, Blanquer D, Togores B, Sauleda J, Perez JL, et al. (2005) Hypermutation is a key factor in development of multiple-antimicrobial resistance in *Pseudomonas aeruginosa* strains causing chronic lung infections. *Antimicrobial Agents and Chemotherapy* 49: 3382-3386.
8. Drenkard E. (2003) Antimicrobial resistance of *Pseudomonas aeruginosa* biofilms. *Microbes and Infection* 5: 1213-1219.

9. Ciofu O, Mandsberg LF, Wang HZ, Hoiby N. (2012) Phenotypes selected during chronic lung infection in cystic fibrosis patients: implications for the treatment of *Pseudomonas aeruginosa* biofilm infections. *Fems Immunology and Medical Microbiology* 65: 215-225.
10. De Kievit TR, Parkins MD, Gillis RJ, Srikumar R, Ceri H, et al. (2001) Multidrug efflux pumps: expression patterns and contribution to antibiotic resistance in *Pseudomonas aeruginosa* biofilms. *Antimicrobial Agents and Chemotherapy* 45: 1761-1770.
11. Robinson C. (1995) The airway epithelium: the origin and target of inflammatory airways disease and injury. *Immunopharmacology of the respiratory system* London: Academic Press 187: 207.
12. Azghani AO. (1996) *Pseudomonas aeruginosa* and epithelial permeability: role of virulence factors elastase and exotoxin A. *American Journal of Respiratory Cell and Molecular Biology* 15: 132-140.
13. Azghani A, Connelly JC, Peterson B, Gray L, Collins M, et al. (1990) Effects of *Pseudomonas aeruginosa* elastase on alveolar epithelial permeability in guinea pigs. *Infection and Immunity* 58: 433.
14. Lee A, Chow D, Haus B, Tseng W, Evans D, et al. (1999) Airway epithelial tight junctions and binding and cytotoxicity of *Pseudomonas aeruginosa*. *American Journal of Physiology-Lung Cellular and Molecular Physiology* 277: L204-L217.
15. Morihara K, Tsuzuki H, Oka T, Inoue H, Ebata M. (1965) *Pseudomonas aeruginosa* elastase. *Journal of Biological Chemistry* 240: 3295.
16. Kipnis E, Sawa T, Wiener-Kronish J. (2006) Targeting mechanisms of *Pseudomonas aeruginosa* pathogenesis. *Medecine et maladies infectieuses* 36: 78-91.
17. Tan MW, Rahme LG, Sternberg JA, Tompkins RG, Ausubel FM. (1999) *Pseudomonas aeruginosa* killing of *Caenorhabditis elegans* used to identify *P. aeruginosa* virulence factors. *Proceedings of the National Academy of Sciences* 96: 2408.

18. Twining SS, Kirschner SE, Mahnke LA, Frank DW. (1993) Effect of *Pseudomonas-aeruginosa* elastase, alkaline protease, and exotoxin-a on corneal proteinases and proteins. *Investigative Ophthalmology & Visual Science* 34: 2699-2712.
19. Azghani A, Bedinghaus T, Klein R. (2000) Detection of elastase from *Pseudomonas aeruginosa* in sputum and its potential role in epithelial cell permeability. *Lung* 178: 181-189.
20. Suter S, Schaad UB, Roux L, Nydegger UE, Waldvogel FA. (1984) Granulocyte neutral proteases and *Pseudomonas* elastase as possible causes of airway damage in patients with cystic fibrosis. *Journal of Infectious Diseases* 149: 523.
21. Clark C, Thomas L, Azghani A. (2011) Inhibition of PKC attenuates *Pseudomonas aeruginosa* elastase induced epithelial barrier disruption. *American Journal of Respiratory Cell and Molecular Biology*.
22. Kuang ZZ, Hao YH, Walling BE, Jeffries JL, Ohman DE, et al. (2011) *Pseudomonas aeruginosa* elastase provides an escape from phagocytosis by degrading the pulmonary surfactant protein-A. *Plos One* 6.
23. Ohman DE, Cryz SJ, Iglewski BH. (1980) Isolation and characterization of a *Pseudomonas aeruginosa* pao mutant that produces altered elastase. *Journal of Bacteriology* 142: 836-842.
24. Woods DE, Cryz SJ, Friedman RL, Iglewski BH. (1982) Contribution of toxin-a and elastase to virulence of *Pseudomonas aeruginosa* in chronic lung infections of rats. *Infection and Immunity* 36: 1223-1228.
25. Citri A, Yarden Y. (2006) EGF-ERBB signalling: towards the systems level. *Nature Reviews Molecular Cell Biology* 7: 505-516.
26. Raimondi F, Santoro P, Barone MV, Pappacoda S, Barretta ML, et al. (2008) Bile acids modulate tight junction structure and barrier function of Caco-2 monolayers via EGFR activation. *American Journal of Physiology-Gastrointestinal and Liver Physiology* 294: G906-G913.

27. Terakado M, Gon Y, Sekiyama A, Takeshita I, Kozu Y, et al. (2011) The Rac1/JNK pathway is critical for EGFR-dependent barrier formation in human airway epithelial cells. *American Journal of Physiology-Lung Cellular and Molecular Physiology* 300: L56-L63.
28. Petecchia L, Sabatini F, Usai C, Caci E, Varesio L, et al. (2012) Cytokines induce tight junction disassembly in airway cells via an EGFR-dependent MAPK/ERK1/2-pathway. *Laboratory Investigation* 92: 1140-1148.
29. Jorissen RN, Walker F, Pouliot N, Garrett TPJ, Ward CW, et al. (2003) Epidermal growth factor receptor: mechanisms of activation and signalling. *Experimental Cell Research* 284: 31-53.
30. Oda K, Matsuoka Y, Funahashi A, Kitano H. (2005) A comprehensive pathway map of epidermal growth factor receptor signaling. *Molecular Systems Biology* 1.
31. Azghani AO, Baker JW, Shetty S, Miller EJ, Bhat GJ. (2002) *Pseudomonas aeruginosa* elastase stimulates ERK signaling pathway and enhances IL-8 production by alveolar epithelial cells in culture. *Inflammation Research* 51: 506-510.
32. Haines JD, Fang J, Fragoso G, Mushynski WE, Almazan G. (2009) Role of the P38 Mapk/Mapk-Activated Protein Kinase 2 (Mk2) Signaling Cascade in Oligodendrocyte Differentiation. *Journal of Neurochemistry* 108: 112-112.
33. Seger R, Krebs EG. (1995) Protein Kinases .7. The Mapk Signaling Cascade. *Faseb Journal* 9: 726-735.
34. Bonni A, Brunet A, West AE, Datta SR, Takasu MA, et al. (1999) Cell survival promoted by the Ras-MAPK signaling pathway by transcription-dependent and -independent mechanisms. *Science* 286: 1358-1362.
35. Wang Y, Zhang J, Yi X, Yu FSX. (2004) Activation of ERK1/2 MAP kinase pathway induces tight junction disruption in human corneal epithelial cells. *Experimental Eye Research* 78: 125-136.

36. Basuroy S, Seth A, Elias B, Naren AP, Rao R. (2006) MAPK interacts with occludin and mediates EGF-induced prevention of tight junction disruption by hydrogen peroxide. *Biochemical Journal* 393: 69-77.
37. Petecchia L, Sabatini F, Varesio L, Camoirano A, Usai C, et al. (2009) Bronchial airway epithelial cell damage following exposure to cigarette smoke includes disassembly of tight junction components mediated by the extracellular signal-regulated kinase 1/2 pathway. *Chest* 135: 1502-1512.
38. Wan H, Winton H, Soeller C, Stewart G, Thompson P, et al. (2000) Tight junction properties of the immortalized human bronchial epithelial cell lines Calu-3 and 16HBE14o. *European Respiratory Journal* 15: 1058-1068.
39. Olivera DS, Boggs SE, Beenhouwer C, Aden J, Knall C. (2007) Cellular mechanisms of mainstream cigarette smoke-induced lung epithelial tight junction permeability changes in vitro. *Inhalation Toxicology* 19: 13-22.
40. Crews CM, Alessandrini A, Erikson RL. (1992) The primary structure of MEK, a protein kinase that phosphorylates the ERK gene product. *Science* 258: 478-480.
41. Romero-Calvo I, Ocon B, Martinez-Moya P, Suarez MD, Zarzuelo A, et al. (2010) Reversible Ponceau staining as a loading control alternative to actin in Western blots. *Analytical Biochemistry* 401: 318-320.
42. Stevenson BR, Siliciano JD, Mooseker MS, Goodenough DA. (1986) Identification of ZO-1: a high molecular weight polypeptide associated with the tight junction (zonula occludens) in a variety of epithelia. *The Journal of Cell Biology* 103: 755-766.
43. Anderson JM, Van Itallie CM. (2009) Physiology and function of the tight junction. *Cold Spring Harbor Perspectives in Biology* 1.
44. Aggarwal S, Suzuki T, Taylor W, Bhargava A, Rao R. (2011) Contrasting effects of ERK on tight junction integrity in differentiated and under-differentiated Caco-2 cell monolayers. *Biochem J* 433: 51-63.
45. Zheng B, Cantley LC. (2007) Regulation of epithelial tight junction assembly and disassembly by AMP-activated protein kinase. *Proceedings of the National Academy of Sciences* 104: 819.

46. Geilen CC, Wieprecht M, Orfanos CE. (1996) The mitogen-activated protein kinases system (MAP kinase cascade): Its role in skin signal transduction. A review. *Journal of Dermatological Science* 12: 255-262.
47. Chen YH, Lu Q, Schneeberger EE, Goodenough DA. (2000) Restoration of tight junction structure and barrier function by down-regulation of the mitogen-activated protein kinase pathway in Ras-transformed Madin-Darby canine kidney cells. *Molecular Biology of the Cell* 11: 849-862.
48. Bell CE, Watson AJ (2013) p38 MAPK regulates cavitation and tight junction function in the mouse blastocyst. *Plos One* 8: 4.
49. Chen ML, Ge ZM, Fox JG, Schauer DB. (2006) Disruption of tight junctions and induction of proinflammatory cytokine responses in colonic epithelial cells by *Campylobacter jejuni*. *Infection and Immunity* 74: 6581-6589.
50. Stuart RO, Nigam SK. (1995) Regulated assembly of tight junctions by protein-kinase C. *Proceedings of the National Academy of Sciences of the United States of America* 92: 6072-6076.
51. Suzuki T, Seth A, Rao R. (2012) Role of phospholipase C gamma-induced activation of protein kinase C epsilon (PKC epsilon) and PKC beta I in epidermal growth factor-mediated protection of tight junctions from acetaldehyde in Caco-2 cell monolayers (vol 283, pg 3574, 2008). *Journal of Biological Chemistry* 287: 6959-6959.
52. Ueda Y, Hirai S, Osada S, Suzuki A, Mizuno K, et al. (1996) Protein kinase C delta activates the MEK-ERK pathway in a manner independent of Ras and dependent on Raf. *Journal of Biological Chemistry* 271: 23512-23519.
53. Axmann A, Seidel D, Reimann T, Hempel U, Wenzel KW. (1998) Transforming growth factor-beta 1-induced activation of the Raf-MEK-MAPK signaling pathway in rat lung fibroblasts via a PKC-dependent mechanism. *Biochemical and Biophysical Research Communications* 249: 456-460.